iScience

CellPress
OPEN ACCESS

Article

Identification of cGAS as an innate immune sensor of extracellular bacterium *Pseudomonas aeruginosa*

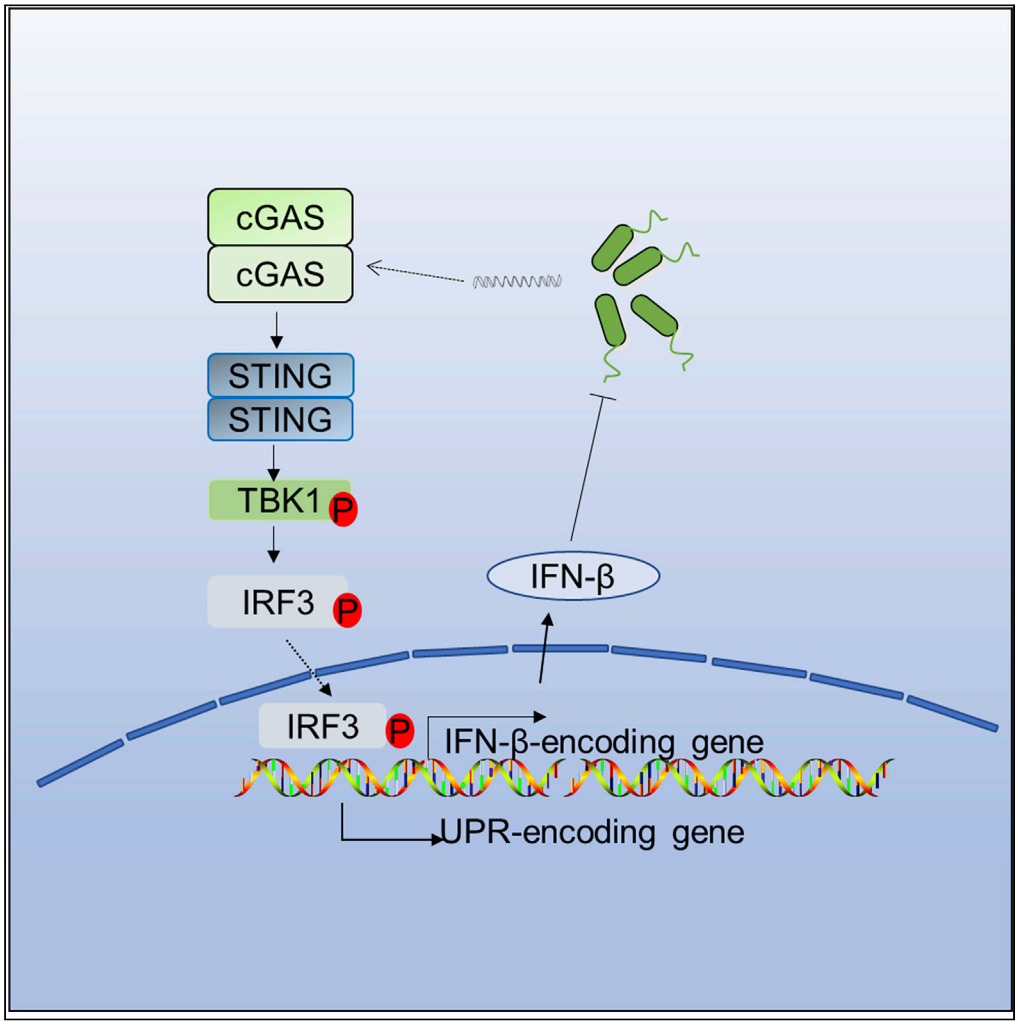

Chuan-min Zhou, Biao Wang, Qun Wu, ..., Qin-qin Pu, Xue-jie Yu, Min Wu

yuxuejie@whu.edu.cn (X.-j.Y.)
min.wu@und.edu (M.W.)

Highlights

The role of cGAS signaling pathway is expanded in sensing extracellular bacteria

cGAS/STING/IFNAR axis is necessary host immunity restricting *P. aeruginosa*

cGAS signaling pathway is involved in modulating unfolded protein response

cGAS is an important nucleic acids' sensor in recognizing extracellular bacteria

Zhou et al., iScience *24*, 101928
January 22, 2021
https://doi.org/10.1016/j.isci.2020.101928

iScience

CellPress
OPEN ACCESS

Article

Identification of cGAS as an innate immune sensor of extracellular bacterium *Pseudomonas aeruginosa*

Chuan-min Zhou,[1,2,3,4] Biao Wang,[2,4] Qun Wu,[2] Ping Lin,[2] Shu-gang Qin,[2] Qin-qin Pu,[2] Xue-jie Yu,[1,*] and Min Wu[2,5,*]

Summary

Cyclic GMP-AMP synthase (cGAS) is reported essential for detecting intracellular bacteria. However, it remains to be determined whether and how cGAS is involved in extracellular bacterial infection. Here, we report that cGAS is essential for mediating type I interferon (IFN) production in infection by multiple extracellular pathogens, including *Pseudomonas aeruginosa*, *Klebsiella pneumoniae*, and *Staphylococcus aureus*. In addition, the canonical cGAS-stimulator of interferon gene (STING)-IFN axis is required for protecting mice from *P. aeruginosa*-induced mouse acute pulmonary infection, confirmed in cGAS pathway-specific gene deficiency mouse models. *cGAS*$^{-/-}$ and *STING*$^{-/-}$ mice exhibited reduced type I IFNs production, excessive inflammatory response accompanied with decreased resistance to *P. aeruginosa* challenge. Unfolded protein response was also modulated by cGAS through IRF3 and type I IFNs under *P. aeruginosa* infection. Collectively, these findings uncover the importance of cGAS in initiating immune responses against extracellular bacterial infection.

Introduction

Nucleic acids are integral parts of pathogens for replication, survival, and invasion and have also been shown as pathogen-associated molecular patterns to trigger innate immune response (Barbalat et al., 2011; Wu and Chen, 2014). To date, various DNA sensors are discovered for the recognition of self- or non-self-nucleic acids, including the endosomal TLR9, and the cytosolic DNA sensors AIM2, cyclic GMP-AMP synthase (cGAS), and IFI16 (Wu and Chen, 2014). Of which, cGAS has recently been identified as a novel DNA sensor responsible for sensing infection of DNA viruses, retroviruses, and intracellular bacteria (Li et al., 2013; Sun et al., 2013; Wu et al., 2013). Upon binding with double-stranded DNA, cGAS is activated and then catalyzes the nucleotide second messenger cyclic AMP-GMP generation, which in turn activates the stimulator of interferon gene (STING) (Gao et al., 2013; Sun et al., 2013). Activated STING is translocated from endoplasmic reticulum (ER) to ER–Golgi intermediate compartment (ERGIC) and Golgi complex triggering TANK-binding kinase 1 (TBK1) and interferon regulatory factor 3 (IRF3) activation and type I IFN production, serving as the important defense mechanism against microbial infection (Wu et al., 2013).

Pseudomonas aeruginosa is an important gram-negative extracellular opportunistic pathogen, which distributes widely in the world. People with immunodeficiency, like cystic fibrosis, burn wounds, chronic obstructive pulmonary disorder, pneumonia, or sepsis, are highly susceptible to *P. aeruginosa* (Cachia and Hodges, 2003; Curran et al., 2018; Miyoshi-Akiyama et al., 2017). Additionally, growing multi-drug resistance makes *P. aeruginosa* extremely difficult to treat (Pang et al., 2019), which has become a significant global public health issue. Neutrophils and macrophages are key components of innate immunity against *P. aeruginosa* attack by promoting inflammatory cytokine production and phagocytosis (Lovewell et al., 2014). It is worth mentioning that that type I IFNs are important for host defense against *P. aeruginosa* infection by modulating multiple innate immune responses such as phagocytosis and RANTES production (Carrigan et al., 2010; Parker et al., 2012; Parker and Prince, 2011). However, little is known about the interaction between cGAS and extracellular bacterium *P. aeruginosa*.

ER is a dynamic intracellular organelle with multiple functions, for instance, maintaining cell homeostasis in response to pathogenic infection (Bettigole and Glimcher, 2015; Grootjans et al., 2016). Currently, three transmembrane proteins (ATF6, PERK, and IRE1) located in the ER lumen are known to detect ER stress,

[1]State Key Laboratory of Virology, School of Health Sciences, Wuhan University, Wuhan 430071, P.R. China

[2]Department of Biomedical Sciences, University of North Dakota, Grand Forks, ND 58203-9037, USA

[3]Zhongnan hospital of Wuhan University, Wuhan, Hubei Province, 430071, P. R. China

[4]These authors contributed equally

[5]Lead contact

*Correspondence: yuxuejie@whu.edu.cn (X.-j.Y.), min.wu@und.edu (M.W.)

https://doi.org/10.1016/j.isci.2020.101928

activating unfolded protein response (UPR). Once activated, these ER stress initiators are dissociated with BiP, a chaperone and master regulator of the UPR, to elicit the UPR process. Although studies indicate that UPR is involved in innate immunity against *P. aeruginosa* infection (Richardson et al., 2010; van 't Wout et al., 2015), it remains largely unknown about the underlying mechanisms of UPR activation.

Here, we demonstrate that DNA sensor cGAS serves as an important sensing mechanism for detecting extracellular bacterial infection. *P. aeruginosa* infection also induced cGAS-STING-IRF3 activation to initiate UPR. To verify that this sensing is a common mechanism, we also tested this phenomenon in other species including *Klebsiella pneumoniae* and *Staphylococcus aureus* and confirmed that cGAS indeed senses a variety of extracellular bacteria in infection. Taken together, we delineate a critical role of cGAS signaling in host immunity against extracellular pathogens.

Results

cGAS is required for *P. aeruginosa*-induced type I IFN response in macrophages

In order to determine the role of cGAS in the infection of the *P. aeruginosa* strain PAO1, the widely used human macrophage cell line THP-1 was infected with PAO1 at different multiplicity of infection (MOI) (1, 2, and 10) and different time points (1 h, 2 h, and 4 h). It is clearly observed that phosphorylation of TBK1 was significantly induced (Figure S1A and S1B). Importantly, p-TBK1 was also activated under UV radiation or heat-killed PAO1 infection (Figure S1C). To solidify our above observation, a mouse macrophage cell line, RAW264.7, was then transfected with RNAi to knockdown the target cGAS and STING genes (Figures S1D–S1G). We observed that transfection of cGAS siRNA or STING siRNA almost abolished the p-IRF3 in RAW264.7 cells following PAO1 infection (Figures S1F and S1G). Reduced p-TBK1 was further confirmed in *STING*$^{-/-}$ RAW264.7 cells (Figure S1I). Immunofluorescence assay showed that cGAS siRNA reduced p-IRF3 nuclear translocation (Figure S1H). Meanwhile, transcription of IRF3 targeted genes (*IFN-β* and *IFIT1*) and production of IFN-β were suppressed in cGAS siRNA- or STING siRNA-treated RAW264.7 cells after PAO1 infection or interferon-stimulatory DNA (ISD) transfection (Figures S2A–S2D). To seek additional evidence, we next used mouse alveolar macrophage (MH-S) cells and observed similar role of cGAS for host detection PAO1 after transfection with cGAS siRNA (Figure S2E). Since primary cells from genetic deficient mice would demonstrate the unequivocal role of cGAS in sensing pathogens, we isolated primary *cGAS*$^{-/-}$ mouse bone marrow-derived macrophages (BMDMs) and found reduced p-IRF3 compared to wild-type (WT) counterparts after PAO1 infection (Figure S2F). Likewise, type I IFN response was also blocked in primary *cGAS*$^{-/-}$ alveolar macrophages and peritoneal macrophages following PAO1 infection (Figures 1A, 1B, S2G, and S2H). To further characterize the roles of cGAS and STING in response to *P. aeruginosa* infection in human macrophages, we utilized CRISPR-Cas9 technique to construct *cGAS*$^{-/-}$, *STING* $^{-/-}$, and *cGAS/STING*$^{-/-}$ THP-1 cells. Consistent with the results observed in mouse macrophages, *cGAS* or *STING* deficiency in THP-1 significantly reduced p-IRF3, transcription of IFN-β, or reduced p-TBK1 (Figures 1C–1F). Additionally, we observed that MyD88 deficiency and phagocytosis inhibitor latrunculin A blocked the activation of IFN signal pathway of IRF3 under PAO1 infection (Figures 1G and 1H). Together, these findings reveal the critical roles of cGAS and STING in promoting type I IFN response under *P. aeruginosa* infection.

The cGAS signaling pathway is responsible for detecting extracellular bacteria *Klebsiella pneumoniae* and *Staphylococcus aureus*

To expand the concept and examine whether cGAS can sense extracellular bacteria in general, we determined whether other extracellular bacteria (*Klebsiella pneumoniae* and *Staphylococcus aureus*) also activate cGAS pathway. Compared with PAO1 infection, deficiency in *cGAS* or *STING* also inhibited p-IRF3 in THP-1 cells (Figure 1I) and type I IFN response in BMDMs (Figures 1J–1L) under *K. pneumoniae* or *S. aureus* infection. Reduced type I IFN response was also noted in STING siRNA-transfected BMDMs (Figures S3A and S3B) under *K. pneumoniae* or *S. aureus* infection and IRF3 siRNA-transfected RAW264.7 cells under PAO1 infection or ISD transfection (Figures S3C and S3D). Therefore, these results indicate that extracellular pathogens *P. aeruginosa*, *K. pneumoniae*, and *S. aureus* are capable of activating type I IFN response in macrophages in a cGAS-pathway-dependent manner.

cGAS is required for sensing *P. aeruginosa*-derived DNA

Next, we set out to perform immunofluorescence assay to elucidate whether the DNA sensor cGAS directly senses *P. aeruginosa* or its genomic DNA. Immunofluorescence assay revealed the colocalization between

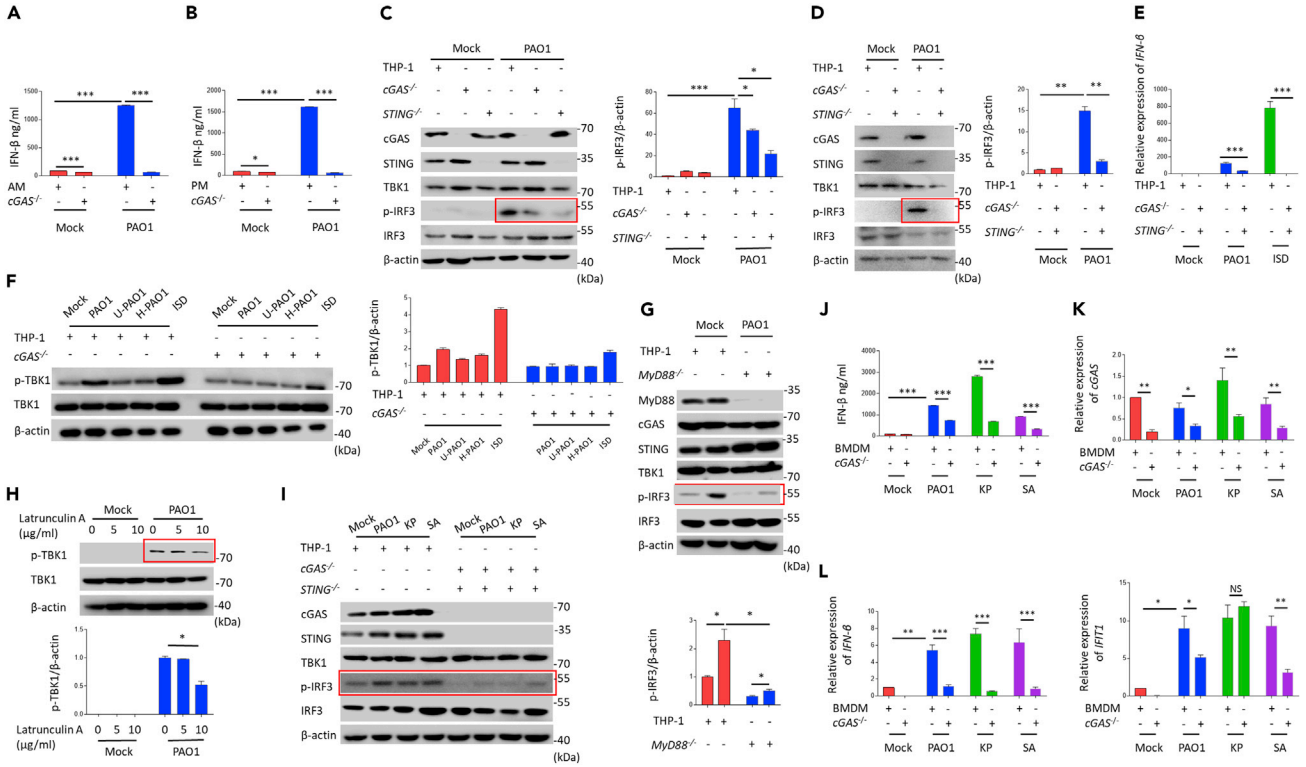

Figure 1. cGAS is required for *Pseudomonas aeruginosa*-induced type I IFN response in macrophages

(A) WT and *cGAS*$^{-/-}$ alveolar macrophages were treated with 10 multiplicity of infection (MOI) PAO1 for 4 h. Cytokine levels of IFN-β in the cell culture supernatant were detected using enzyme-linked immunosorbent assay (ELISA) .

(B) WT and cGAS$^{-/-}$ peritoneal macrophages were treated with 10 MOI PAO1 for 4 h. Cytokine levels of IFN-β in the cell culture supernatant were detected using ELISA.

(C and D) cGAS$^{-/-}$ and STING$^{-/-}$ THP-1 cells were treated with 10 MOI PAO1 for 4 h. Immunoblot analysis of cGAS signaling pathways.

(E) WT and cGAS$^{-/-}$ STING$^{-/-}$ THP-1 cells were treated with 10 MOI PAO1 or ISD for 4 h. qPCR measuring mRNA levels of IFN-β in WT and cGAS$^{-/-}$ STING$^{-/-}$ THP-1 cells.

(F) WT and *cGAS*$^{-/-}$ THP-1 cells were treated with 10 MOI PAO1, UV-PAO1, and PAO1 DNA for 4 h. qPCR was performed to measure mRNA levels of IFN-β.

(G) WT and *MyD88*$^{-/-}$ THP-1 cells were treated with 10 MOI PAO1 for 4 h. Immunoblot analysis of cGAS signaling pathways.

(H) WT THP-1 cells were pre-treated with phagocytosis inhibitor latrunculin A and then treated with 10 MOI PAO1, *K. pneumoniae*, and *S. aureus* for 4 h. qPCR was performed to measure mRNA levels of IFN-β.

(I) WT and *cGAS*$^{-/-}$ *STING*$^{-/-}$ THP-1 cells were treated with 10 MOI PAO1, *K. pneumoniae*, and *S. aureus* for 4 h. Immunoblot analysis of cGAS signaling pathways.

(J) WT and cGAS$^{-/-}$ BMDMs were treated with 10 MOI PAO1, *K. pneumoniae*, and *S. aureus* for 4 h. Cytokine levels of IFN-β in the cell culture supernatant were detected using ELISA.

(K) WT and cGAS$^{-/-}$ BMDMs were treated with 10 MOI PAO1, *K. pneumoniae*, and *S. aureus* for 4 h. qPCR measuring mRNA levels of cGAS in WT and cGAS$^{-/-}$ BMDMs.

(L) WT and cGAS$^{-/-}$ BMDMs were treated with 10 MOI PAO1, *K. pneumoniae*, and *S. aureus* for 4 h. qPCR was performed to measure mRNA levels of IFN-β or *IFIT1*.

ELISA and qPCR data (mean ± standard error of mean (SEM)) are representative of three independent experiments (*p ≤ 0.05, **p ≤ 0.01, ***p ≤ 0.001 one-way analysis of variance (ANOVA) with Tukey post hoc test).

cGAS and PAO1-GFP in macrophages (Figure 2A). Colocalization between cGAS and *PAO1* genomic DNA, which was pre-labeled with a thymidine analog 5-ethynyl-2′-deoxyuridine, was also observed in the BMDM cytoplasm (Figure 2B). To further confirm the role of DNA in activating cGAS under *P. aeruginosa* infection, *P. aeruginosa* genomic DNA was isolated, and we found that *P. aeruginosa* genomic DNA transfection is capable of activating type I IFN response which was abolished in cGAS siRNA-transfected RAW264.7 cells and *cGAS*$^{-/-}$ BMDMs (Figures 2C–2E). Critically, DNase pretreatments were found to block the type I IFN response induced by PAO1 infection and genomic DNA transfection, respectively (Figures 2F and 2G), indicating that direct contact of bacterial DNA is critical to initiate host defense via cGAS sensing. We next used co-immunoprecipitation (Co-IP) to determine whether cGAS could bind PAO1 genomic DNA directly

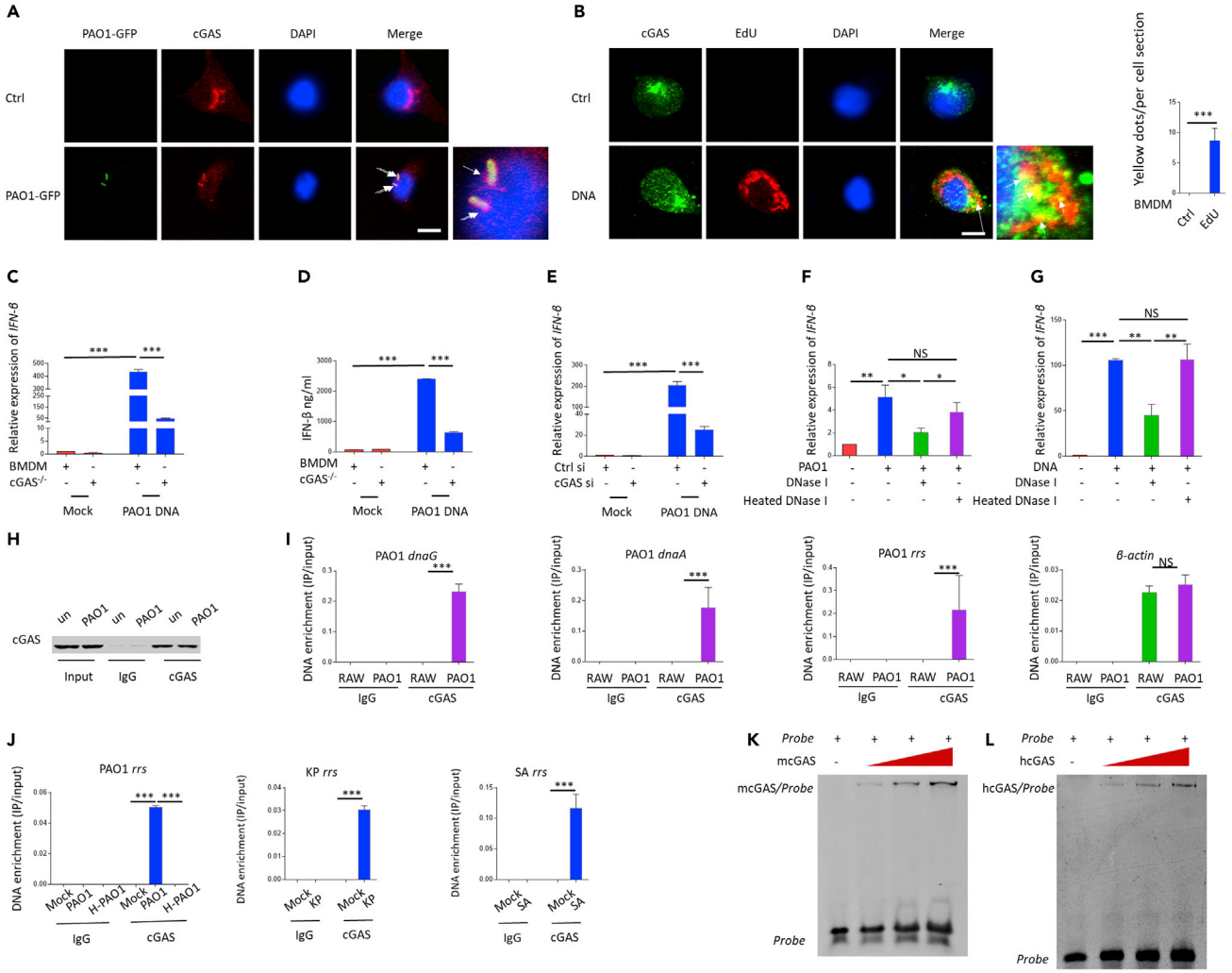

Figure 2. cGAS is required for sensing *P. aeruginosa*-derived DNA

(A) Colocalization of PAO1-GFP (green) with cGAS (red) in BMDMs. Scale bar, 5 μm.

(B) Colocalization of PAO1 genomic DNA (red) with cGAS (green) in BMDMs. Scale bar, 5 μm.

(C) WT and cGAS$^{-/-}$ BMDMs were transfected with PAO1 genomic DNA for 4 h. qPCR was performed to measure mRNA levels of IFN-β.

(D) WT and cGAS$^{-/-}$ BMDMs were transfected with PAO1 genomic DNA for 4 h. Cytokine levels of IFN-β in the cell culture supernatant were detected using ELISA.

(E) RAW264.7 cells were transfected with control siRNA or cGAS siRNA for 48 h and then transfected with PAO1 genomic DNA for 4 h. mRNA levels of *IFN-β* were detected.

(F) BMDMs were infected with 10 MOI PAO1 for 4 h with or without DNase I or heated DNase I. qPCR was performed to measure mRNA levels of IFN-β.

(G) BMDMs were transfected with PAO1 DNA with or without DNase I or heated DNase I for 4 h. qPCR was performed to measure mRNA levels of IFN-β.

(H) Immunoblotting of lysates of RAW264.7 cells infected by PAO1 or PBS, then immunoprecipitated with IgG or cGAS antibody, assessed with anti-cGAS. Total cell lysates (TCLs) were applied for immunoblotting analysis as a control.

(I) qPCR of PAO1 genes and mouse β-Actin from DNA samples isolated from cGAS IPs in uninfected or infected RAW264.7 cells. PAO1 gene levels were normalized to inputs.

(J) qPCR of PAO1, *K. pneumoniae*, or *S. aureus* genes and human β-actin from DNA samples isolated from cGAS IPs in uninfected or infected THP-1 cells. Gene levels were normalized to inputs.

(K) EMSA for binding of mcGAS to PAO1 rrs probe.

(L) EMSA for binding of hcGAS to PAO1 *rrs* probe.

ELISA and qPCR data (mean ± SEM) are representative of three independent experiments (*p ≤ 0.05, **p ≤ 0.01, ***p ≤ 0.001 one-way ANOVA with Tukey post hoc test).

during infection. RAW264.7 cells infected with PAO1 were immunoprecipitated with cGAS antibody (Figure 2H). The abundance of several PAO1 genes including *dnaA*, *dnaG*, and *rrs*, which are important for bacterial DNA replication, was measured by quantitative polymerase chain reaction (qPCR). Interestingly, we observed that these DNA sequences were significantly enriched by cGAS in infected cells compared to the uninfected controls (Figure 2I). In contrast, no significant change in the abundance of host-derived DNA sequence of *β-actin* was observed (Figure 2I). Additional data indicated that cGAS is capable of binding PAO1, *K. pneumoniae*, and *S. aureus*-derived DNA in THP-1 cells, while cGAS cannot bind PAO1 DNA under heat-killed PAO1 infection (Figure 2J). To further investigate the direct binding affinity of cGAS and PAO1-derived DNA, we then purified His-tagged mcGAS protein using pet-28a expression system. PAO1 rrs probe was obtained by PCR. cGAS was shown to bind the probe as determined by an electrophoretic molecular shift assay (EMSA) (Figure 2K). Similar results were also observed using hcGAS protein (Figure 2L). Taken together, these studies illustrate that cGAS is involved in sensing extracellular bacteria-derived DNA under infection.

cGAS deficiency impairs the activation of ER stress after *P. aeruginosa* infection

It is known that UPR is involved in innate immunity against *P. aeruginosa* infection. To unveil the mechanism by which cGAS senses and initiates host immunity against PAO1 infection, we speculate that UPR may be involved in the process as they are linked to the PAO1 infection in previous studies (Richardson et al., 2010; van 't Wout et al., 2015). In agreement with previous studies, PAO1 infection was capable of activating UPR pathway (Figure S4A). Intriguingly, activation of UPR was impaired in cGAS siRNA-transfected RAW264.7 cells in response to infection of PAO1 and transfection of ISD (Figure 3A). *cGAS* deficiency decreased the transcription of *BiP*, *ATF4*, and *XBP1-S* (Figures S4B–S4D). To further define the biological relevance, we next investigated the role of cGAS in primary BMDMs and lung samples isolated from WT and *cGAS*$^{-/-}$ mice. *cGAS*$^{-/-}$ BMDMs and lung samples showed reduced UPR after PAO1 infection (Figures 3B and 3C). Furthermore, a similar immunoblotting pattern was observed in IRF3 siRNA-treated RAW264.7 cells (Figure 3D). Furthermore, we found that activation of UPR following PAO1 infection was significantly blocked in the lung of *IFNAR*$^{-/-}$ mice (Figure 3E). Together, cGAS impacts ER stress through sensing PAO1.

cGAS-IRF3-IFN axis is required for *P. aeruginosa*-induced unfolded protein response

Although cGAS is important for mediating *PAO1*-induced UPR, the detailed mechanism is still unclear. In view of that cGAS is dependent on IRF3-modulated downstream signals, we hypothesized that IRF3, which is known as the dominant transcription factor for induction of numerous genes (Yanai et al., 2012), may be involved in the process of UPR activation. To elaborate the role of IRF3 in modulating UPR, we performed analysis of the public chromatin immunoprecipitation sequencing (ChIP-seq) data set using bioinformatics approaches. Enriched IRF3 binding sites were found in the promoter region of *BiP* (−700 to −400) and *ATF4* (−590 to −290) (Figures 4A and 4B). To this end, we posit that transcription of *BiP* and *ATF4* may be regulated by IRF3. To assess the binding affinity of IRF3 to *BiP* and *ATF4* promoters, we performed ChIP assay with IRF3-specific antibody and normal rabbit IgG as a control under PAO1 infection. Our ChIP-PCR data showed that the promoter regions of *BiP* and *ATF4* were significantly enriched in the IRF3 antibody group but not in the IgG isotype group, providing direct proof of the recruitment of IRF3 to *BiP* and *ATF4* promoters (Figures 4C and 4D). To further assess the molecule mechanism of IRF3-mediated transcription of *BiP* and *ATF4*, we constructed luciferase vectors containing *BiP* and *ATF4* promoters. Our analysis showed that luciferase expression in RAW264.7 cells was inhibited in IRF3 siRNA-treated groups (Figure 4E, 4F and S5A), indicating that mRNA transcription of *BiP* and *ATF4* was regulated by IRF3. We also noted reduced expression of *BiP* and *ATF4* in IRF3 siRNA-transfected RAW264.7 cells compared to siNC-transfected RAW264.7 cells (Figures 4G and 4H). Comparable results were also observed in STING KO RAW264.7 cells (Figures S5B–S5D). Mechanistically, we delineate that transcription of UPR-related molecules *BiP* and *ATF4* was enhanced by IRF3 by directly binding to their promoters.

Now that type I IFNs are downstream of cGAS-STING, we next investigated whether type I IFNs, especially IFN-α and IFN-β, influence the activation of UPR. We found that the ER chaperone protein BiP was strongly induced in response to type I IFNs treatment in both BMDMs and RAW264.7 cells (Figures 4I, 4J, and S6A–S6D). Critically, immunoblotting also showed that type I IFN treatment not only activated ATF4 pathway but also induced additional signaling pathways in a time-dependent manner (Figures S6D, 4I, and 4J). Moreover, we showed that IFN-γ also activated all 3 UPR pathways similar to type I IFNs (Figures S6E, S6F, 4I, and 4J). Our data also suggest that ATF6, ATF4, and XBP1 were activated and translocated into the nucleus

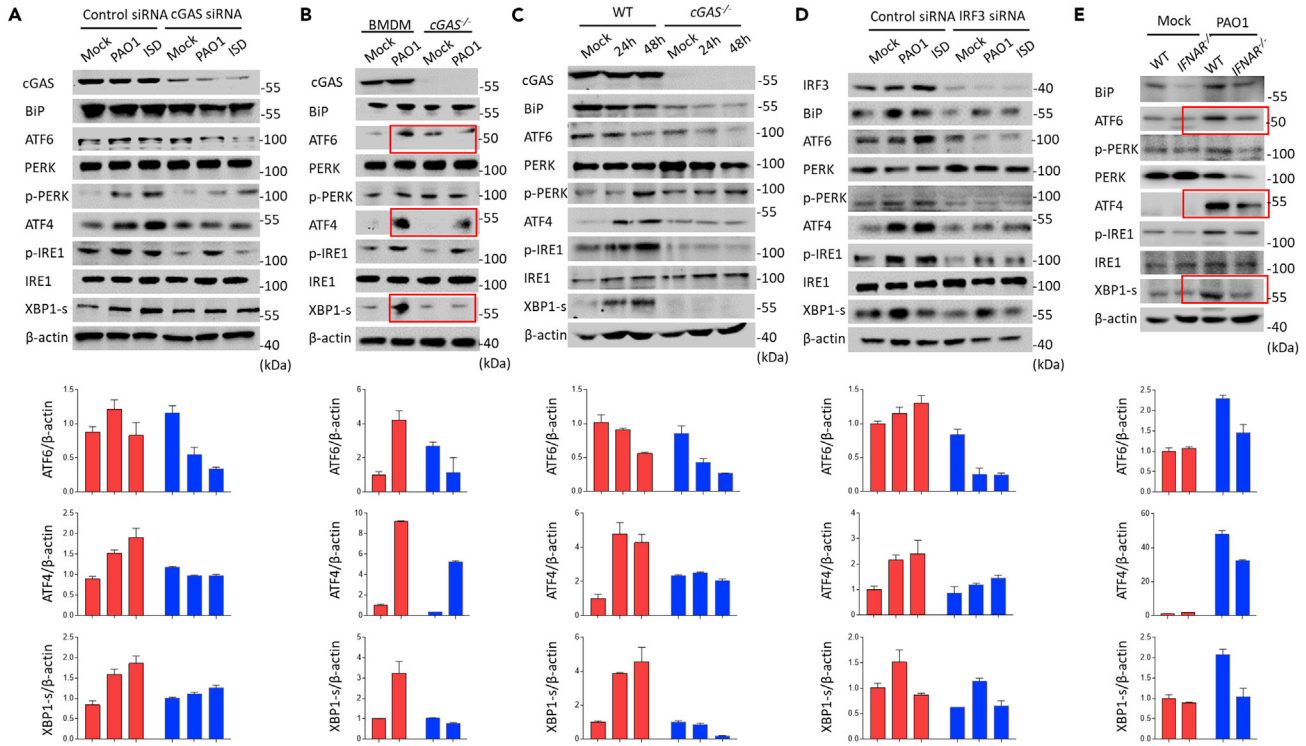

Figure 3. *cGAS* deficiency impairs the activation of ER stress induced by *P. aeruginosa* infection

(A) RAW264.7 cells were transfected with control siRNA or cGAS siRNA and then treated with 10 MOI PAO1 or ISD for 4 h. Immunoblotting analysis of UPR signaling pathways.

(B) WT and *cGAS*$^{-/-}$ BMDMs were treated with 10 MOI PAO1 or ISD for 4 h. Immunoblotting analysis of UPR signaling pathways.

(C) WT and cGAS$^{-/-}$ mice were infected with PAO1 for 24 or 48 h. Immunoblotting analysis of UPR signaling pathways in mouse lung samples.

(D) RAW264.7 cells were transfected with control siRNA or IRF3 siRNA and then treated with 10 MOI PAO1 or ISD for 4 h. Immunoblotting analysis of UPR signaling pathways.

(E) WT and *IFNAR*$^{-/-}$ mice were infected with PAO1 for 48 h. Immunoblotting analysis of UPR signaling pathways in mouse lung samples.

ELISA and qPCR data (mean ± SEM) are representative of three independent experiments (*$p \leq 0.05$, **$p \leq 0.01$, ***$p \leq 0.001$ one-way ANOVA with Tukey post hoc test).

after IFN treatment, which was comparable to Tg treatment (Figure S6G). We then used siRNA to knock down STAT1, STAT2, and IRF9, respectively (Figure S6H). Immunoblotting analysis showed that silencing of STAT1, STAT2, and IRF9 significantly blocked IFN-induced UPR (Figure 4K). To further elucidate whether interferon-stimulated gene factor 3 (ISGF3) may function in modulating the UPR directly, we analyzed STAT1-ChIP-seq data and noticed that there was no binding affinity between STAT1 to *BiP* and *ATF4* promoters (Figures S6I and S6J), indicating that ISGF3 may not directly regulate the transcription of *BiP* and *ATF4*. Although the detailed mechanism remains to be studied, these data confirm that type I IFNs play important roles in modulating UPR.

cGAS protects against *P. aeruginosa* in pulmonary infection

Increasing evidence supports that cGAS is involved in intracellular bacterial infection both *in vitro* and *in vivo* (Hansen et al., 2014; Wassermann et al., 2015; Watson et al., 2015). The cGAS signaling pathway is also important for restricting infection of multiple intracellular pathogens to maintain host homeostasis. To elaborate the protective role of cGAS in extracellular bacterial infection *in vivo*, an acute pulmonary infection model was established through intranasal instillation of 0.5×10^7 CFU PAO1 in C57BL/6J WT, *cGAS*$^{-/-}$ and *STING*$^{-/-}$ mice. We noticed that PAO1-infected *cGAS*$^{-/-}$ and *STING*$^{-/-}$ mice exhibited increased lethality (Figures 5A and 5B) and increased bacterial burdens compared to WT mice (Figures S7A and S7B). To further define how cGAS functions in limiting PAO1 pathogenesis, lung pathological changes were detected in both *cGAS*$^{-/-}$ and *STING*$^{-/-}$ mice. Lungs of *cGAS*$^{-/-}$ *STING*$^{-/-}$ mice showed severe tissue injury compared to WT mice (Figure 5C). Additionally, infection of PAO1 in *cGAS*$^{-/-}$ mice led to decreased type I IFN levels compared to WT mice, indicating that IFN pathways were partially

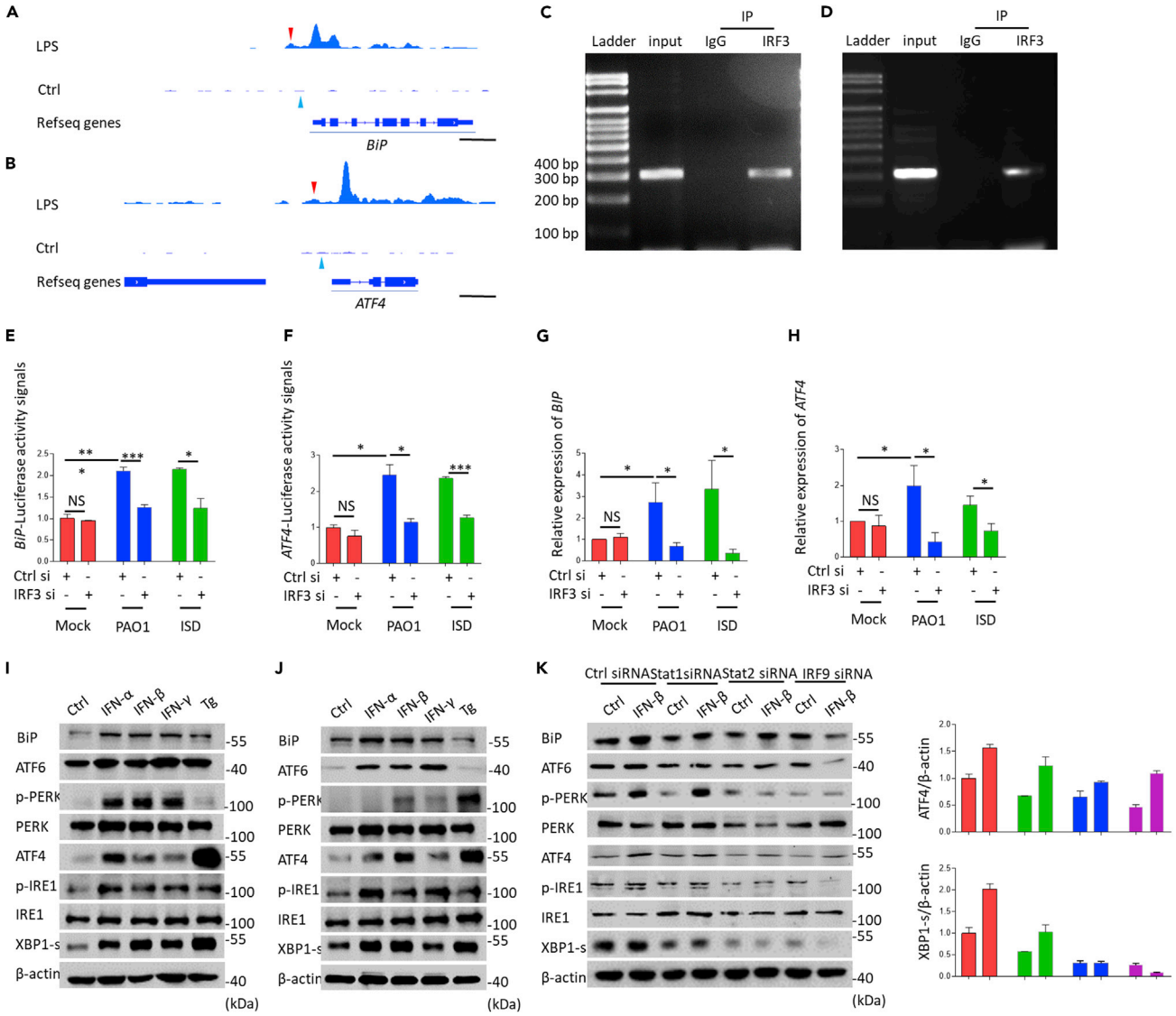

Figure 4. cGAS-IRF3-IFN axis is required for *P. aeruginosa*-induced unfolded protein response

(A and B) Chromatin immunoprecipitation sequencing (ChIP-seq) for IRF3 binding in BiP, ATF4 normalized by input. Red arrows indicate the IRF3 binding region. Blue arrows indicate transcription start site (TSS) of *BiP* or *ATF4*. Scale bar, 1000 bp.

(C and D) ChIP-qPCR detecting the *BiP* or *ATF4* promoters in BMDMs.

(E and F) Control siRNA or IRF3 siRNA-treated RAW264.7 cells were pre-transfected with *BiP* or *ATF4* luciferase vectors for 24 h and then treated with 10 MOI PAO1 or ISD for 4 h. Luciferase activity was detected using Dual-Luciferase Reporter Assay System.

(G and H) RAW264.7 cells were transfected with control siRNA or IRF3 siRNA and then treated with 10 MOI PAO1 or ISD for 4 h. qPCR measured mRNA levels of *BiP* or *ATF4*.

(I) RAW264.7 cells were treated with IFN-α, IFN-β, IFN-γ, and Tg for 6 h. Immunoblotting analysis of UPR signaling pathways.

(J) BMDMs were treated with IFN-α, IFN-β, IFN-γ, and Tg for 6 h. Immunoblotting analysis of UPR signaling pathways.

(K) RAW264.7 cells were transfected with control siRNA, STAT1 siRNA, STAT2 siRNA, or IRF9 siRNA and then treated with IFN-β for 6 h. Immunoblotting analysis of UPR signaling pathways.

ELISA and qPCR data (mean ± SEM) are representative of three independent experiments (*$p \leq 0.05$, **$p \leq 0.01$, ***$p \leq 0.001$ one-way ANOVA with Tukey post hoc test).

blocked (Figures 5D and 5E). *cGAS*$^{-/-}$ and *STING*$^{-/-}$ mice also showed higher production of non-type I IFN inflammatory cytokines than those in WT mice (Figures 5F and 5G). Moreover, *IFNAR*$^{-/-}$ mice also exhibited severe lung injury compared to WT mice (Figure 5C). Collectively, these findings affirm that cGAS has an essential role in defending against extracellular pathogens such as *P. aeruginosa* in the acute pulmonary infection model.

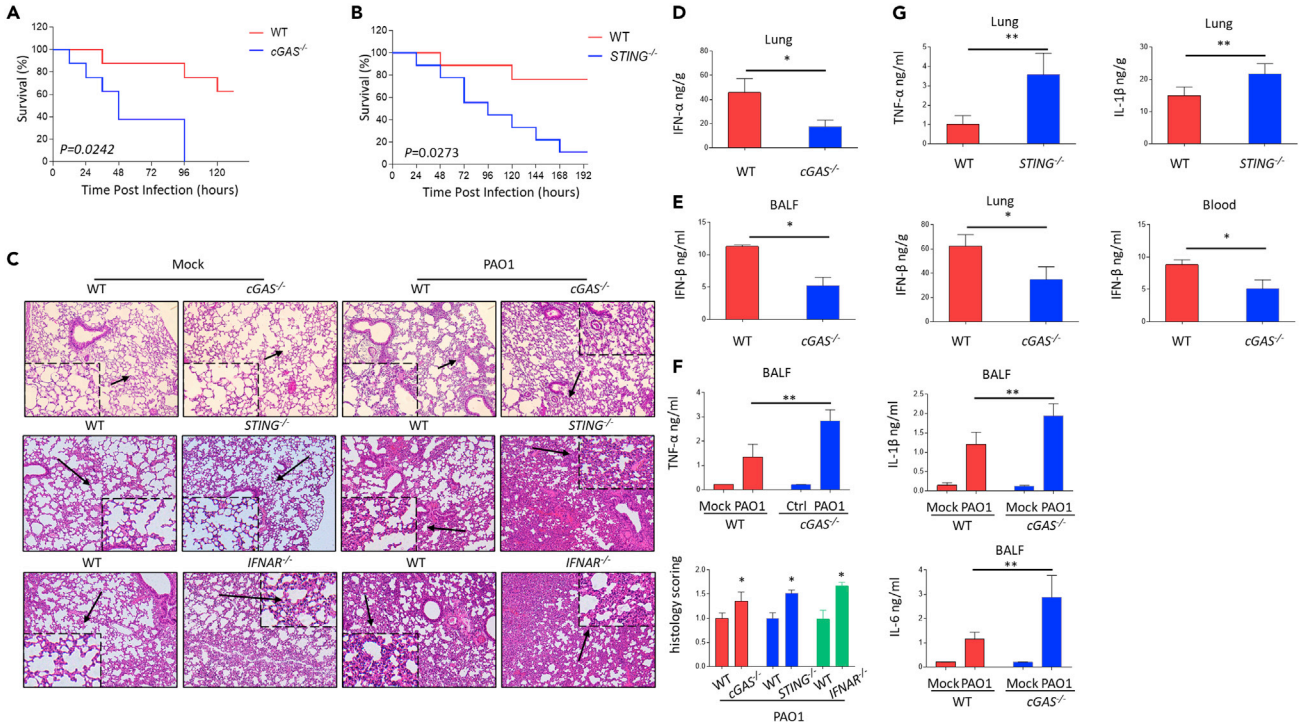

Figure 5. cGAS protects mice against *P. aeruginosa* in pulmonary infection

(A) C57BL/6J WT and *cGAS*$^{-/-}$ mice were challenged with 0.5 × 10^7 CFU PAO1. Survival of mice was monitored up to 7 days. Kaplan-Meier survival curves were obtained using GraphPad. p = 0.0242.

(B) C57BL/6J WT and STING$^{-/-}$ mice were challenged with 0.5 × 10^7 CFU PAO1. Survival of mice was monitored up to 8 days. Kaplan-Meier survival curves were obtained using GraphPad. p = 0.0273.

(C) Pathology of WT, cGAS$^{-/-}$, STING$^{-/-}$, and IFNAR$^{-/-}$ mice in response to PAO1 infection. H&E staining of lung sections from mice. Original magnification ×200.

(D) ELISA analyzes cytokine levels of IFN-α in WT and *cGAS*$^{-/-}$ mice lung.

(E) ELISA analyzes cytokine levels of TNF-α, IL-1β, and IL-6 in in WT and *cGAS*$^{-/-}$ mice lung BALF.

(F) ELISA analyzes cytokine levels of IFN-β in WT and *cGAS*$^{-/-}$ mice BALF, lung, and blood.

(G) ELISA analyzes cytokine levels of TNF-α and IL-1β in WT and *STING*$^{-/-}$ mice lung.

ELISA and qPCR data (mean ± SEM) are representative of three independent experiments (*p ≤ 0.05, **p ≤ 0.01, ***p ≤ 0.001 one-way ANOVA with Tukey post hoc test).

Discussion

Viral and intracellular bacterial pathogens are well established to be sensed by cGAS-mediated immune defense (Hansen et al., 2014; Lahaye et al., 2013; Ma et al., 2015; Wassermann et al., 2015; Watson et al., 2015). Although a previous study has confirmed that group B streptococcus promoted the activation of cGAS (Andrade et al., 2016), the entire cGAS sensing pathways and molecular mechanisms have not been postulated and confirmed systematically in sensing extracellular bacteria. Here, our data demonstrate systemically the key role of cGAS signaling pathway in sensing extracellular bacterium *P. aeruginosa* invasion.

While *P. aeruginosa* is early considered an extracellular bacterium (Sadikot et al., 2005), multiple studies confirmed the penetration of *P. aeruginosa* into host cells, which has been maintained over the course of *P. aeruginosa* evolution. *P. aeruginosa* may be able to enter nonphagocytic cells, which relies on the interaction between T6SS effector VgrG2b and γTuRC (Chi et al., 1991; Sana et al., 2012, 2015). After injection into cells, invading *P. aeruginosa* may be sensed by DNA sensor cGAS directly via targeting *P. aeruginosa* genomic DNA, which was supported by our cGAS Co-IP assay. Additionally, our immunofluorescence data also indicated the significant colocalization between cGAS and *P. aeruginosa* genomic DNA, despite not overwhelming, suggesting that the process of signaling is dynamic and spatial temporarily imbalanced. Additionally, phagocytosis inhibitors blocked the activation of TBK1, which indicates

that *P. aeruginosa* internalization may be essential for mediating type I IFN response. However, the detailed mechanism is not clear and warrants further investigation whether *P. aeruginosa* internalization effectors and T6SS are involved in cGAS activation. Based on these studies, we suggest that *P. aeruginosa* be considered a unique quasi extracellular bacterium. It is worth mentioning that outer membrane vesicles (OMVs) derived from multiple gram-negative bacteria are important in host-pathogen interactions and also contain nucleic acids (Bitto et al., 2017). Hence, it is interesting to further investigate the interaction of OMVs and cGAS signal pathway. Additionally, release of mtDNA was confirmed capable of activating cGAS pathway under several microbe infection models (Aguirre et al., 2017; McArthur et al., 2018; Sun et al., 2017; Zheng et al., 2018). Though our evidence suggests that cGAS binds to bacterial DNA during *P. aeruginosa* infection, we cannot rule out the involvement of other host DNA agonists, like mtDNA.

Apart from cGAS, many pattern recognition receptors (PRRs) were reported to be involved in type I IFN response, such as membrane and endosome Toll-like receptors (TLRs), cytoplasmic RNA sensor RIG-I and MDA5, and novel nuclear DNA sensor hnRNPA2B1 (Anthoney et al., 2018; Wang et al., 2019; Wu and Chen, 2014). Of the various PRRs, TLRs were the most characterized to be involved in detecting bacterial infection. It is known that membrane TLR2 mainly functions by sensing gram-positive bacterial diacylated lipopeptides, while TLR4 recognizes the gram-negative bacterial LPS, and TLR5 senses bacterial flagellin. Endosomal TLR9 serves as cellular PRRs by detecting bacterial unmethylated CpG-containing DNA, whereas TLR3 and TLR8 are involved in responding to double-stranded RNA and single-stranded RNA, respectively. These studies support that the sensing pathways for TLRs may be extremely heterogenic and varied with pathogen strains and species, as well as their particular components. Hence, we propose that the recognition of pathogens may be not solely dependent on one pathway, complementary and somewhat redundant mechanisms may serve to strengthen the innate immunity to achieve robust and dynamic response. Here, we also found that type I IFN response induced by *P. aeruginosa* infection is significantly but only partially blocked in *cGAS*$^{-/-}$ mice and cells, supporting that cGAS and TLR (TLR4 or TLR9)/MYD88 pathways may also be involved in host defense together against *P. aeruginosa* by inducing type I IFN production (Huang et al., 2005; Parker et al., 2012).

P. aeruginosa is shown capable of activating UPR, which is reported to be essential for host defense against *P. aeruginosa* infection (Richardson et al., 2010; van 't Wout et al., 2015). To date, different studies demonstrate that activation of ER stress promotes the type I IFN response mediated by STING (Liu et al., 2012; Petrasek et al., 2013). Here, we observed that *P. aeruginosa* infection-induced UPR is associated with the cGAS signaling pathway, supporting the data that STING is shown to influence UPR (Guimaraes et al., 2019; Moretti et al., 2017; Wu et al., 2019). Additionally, we reveal that cGAS was necessary for inducing UPR in an IRF3-dependent fashion as a potentially upstream regulator of UPR. IRF3 was shown to interact with *BiP* and *ATF4* promoters using ChIP-seq analysis. We then reasoned that type I IFNs may mediate UPR activation under *P. aeruginosa* infection. We noticed that type I IFNs were able to activate UPR. Furthermore, *IFNAR*$^{-/-}$ deficiency blocked the activation of UPR in response to *P. aeruginosa* infection in mice.

It is well accepted that type I IFN is key in antiviral replication. However, the interaction of type I IFNs with bacteria seems somewhat pleiotropic and unpredictable (Boxx and Cheng, 2016; Manzanillo et al., 2012; Yamashiro et al., 2020). Here, by using multiple KO mice lacking cGAS or its related signals, we clearly identified an important role of cGAS signaling pathway against *P. aeruginosa* infection. Critically, we revealed that *cGAS*$^{-/-}$ and *STING*$^{-/-}$ mice exhibited heightened mortality, severe lung injury, impaired type I IFNs, and increased inflammatory cytokines in lungs compared to WT mice. In particular, *IFNAR*$^{-/-}$associated lung injury, as well as cGAS and STING KO phenotypes, also reflects that the cGAS-STING-IFN axis is critical for host defense in extracellular pathogens, supporting the role of type I IFNs in restricting the attack of *P. aeruginosa* infection (Carrigan et al., 2010; Parker et al., 2012; Parker and Prince, 2011).

The cGAS signaling pathway was shown to positively modulate inflammatory response through NF-κB. However, STING has been previously shown as an anti-inflammatory molecule by inhibiting p38, JNK, ERK, and NF-κB activity in a keratitis model (Chen et al., 2018). Here, our studies further investigated the role of the cGAS-STING axis in inflammatory responses and confirmed that *cGAS*$^{-/-}$ and *STING*$^{-/-}$ mice exacerbated enhanced inflammatory response under *P. aeruginosa* infection, indicating that the cGAS

signaling axis acted as a negative regulator of inflammatory function in this particular *P. aeruginosa* infection mouse model.

In summary, we identified cGAS as a DNA sensor for detecting and restricting extracellular pathogen *P. aeruginosa* by promoting the production of type I IFNs, which may be a general mechanism in a variety of bacterial infections. IRF3 and type I IFNs are shown to trigger the activation of UPR pathways. Our study expands the list of pathogens to be sensed by cGAS and identified the related mechanism involving UPR in protective processes occurring in both cell and mouse infection models.

Limitations of the study

In this study, we identify the cGAS as an important DNA sensor for recognizing and restricting *P. aeruginosa* infection. However, we also made a number of interesting observations remaining further investigation. How does *P. aeruginosa* release or inject its genomic DNA into cell plasma for cGAS recognition? Is it dependent on T6SS? Furthermore, is endosomal DNA receptor TLR9 involved in sensing *P. aeruginosa* infection? Whether mtDNA is recognized by cGAS under *P. aeruginosa* infection? Answering those questions is important for understanding DNA sensor and *P. aeruginosa* interaction, providing a basis for future research.

Resource availability

Lead contact

Min Wu, Department of Biomedical Sciences, University of North Dakota, Grand Forks, North Dakota 58203-9037, USA; email: min.wu@med.und.edu.

Materials availability

All related information or materials generated in this study are available upon request.

Data and code availability

This study did not involve code generation.

Methods

All methods can be found in the accompanying Transparent methods supplemental file.

Supplemental information

Supplemental information can be found online at https://doi.org/10.1016/j.isci.2020.101928.

Acknowledgments

This project was supported by National Institutes of Health of USA 364 (R01 AI109317-04 and R01 AI138203-01 to M.W.). We thank UND imaging core for confocal imaging supported by NIH grants INBRE P20GM103442 and P20GM113123. We also thank Dr. H.W. Virgin and Dr. Charles Rice for kindly providing *cGAS*$^{-/-}$ mice.

Author contributions

C.M.Z. performed the experiment, data analysis, and wrote the manuscript; B.W., P.L., Q.W., S.G.Q., and Q.Q.P. assisted in data analysis and some experiments; M.W. and C.M.Z. conceived of the study and revised the manuscript; X.J.Y. revised the manuscript.

Declaration of interests

The authors declare no competing interests.

Received: June 23, 2020
Revised: October 22, 2020
Accepted: December 4, 2020
Published: January 22, 2021

References

Aguirre, S., Luthra, P., Sanchez-Aparicio, M.T., Maestre, A.M., Patel, J., Lamothe, F., Fredericks, A.C., Tripathi, S., Zhu, T., Pintado-Silva, J., et al. (2017). Dengue virus NS2B protein targets cGAS for degradation and prevents mitochondrial DNA sensing during infection. Nat. Microbiol. *2*, 17037.

Andrade, W.A., Firon, A., Schmidt, T., Hornung, V., Fitzgerald, K.A., Kurt-Jones, E.A., Trieu-Cuot, P., Golenbock, D.T., and Kaminski, P.A. (2016). Group B Streptococcus degrades cyclic-di-AMP to modulate STING-dependent type I interferon production. Cell Host Microbe *20*, 49–59.

Anthoney, N., Foldi, I., and Hidalgo, A. (2018). Toll and Toll-like receptor signalling in development. Development *145*, dev156018.

Barbalat, R., Ewald, S.E., Mouchess, M.L., and Barton, G.M. (2011). Nucleic acid recognition by the innate immune system. Annu. Rev. Immunol. *29*, 185–214.

Bettigole, S.E., and Glimcher, L.H. (2015). Endoplasmic reticulum stress in immunity. Annu. Rev. Immunol. *33*, 107–138.

Bitto, N.J., Chapman, R., Pidot, S., Costin, A., Lo, C., Choi, J., D'Cruze, T., Reynolds, E.C., Dashper, S.G., Turnbull, L., et al. (2017). Bacterial membrane vesicles transport their DNA cargo into host cells. Sci. Rep. *7*, 7072.

Boxx, G.M., and Cheng, G. (2016). The roles of type I interferon in bacterial infection. Cell Host Microbe *19*, 760–769.

Cachia, P.J., and Hodges, R.S. (2003). Synthetic peptide vaccine and antibody therapeutic development: prevention and treatment of Pseudomonas aeruginosa. Biopolymers *71*, 141–168.

Carrigan, S.O., Junkins, R., Yang, Y.J., Macneil, A., Richardson, C., Johnston, B., and Lin, T.J. (2010). IFN regulatory factor 3 contributes to the host response during Pseudomonas aeruginosa lung infection in mice. J. Immunol. *185*, 3602–3609.

Chen, K., Fu, Q., Liang, S., Liu, Y., Qu, W., Wu, Y., Wu, X., Wei, L., Wang, Y., Xiong, Y., et al. (2018). Stimulator of interferon genes promotes host resistance against Pseudomonas aeruginosa keratitis. Front. Immunol. *9*, 1225.

Chi, E., Mehl, T., Nunn, D., and Lory, S. (1991). Interaction of Pseudomonas aeruginosa with A549 pneumocyte cells. Infect. Immun. *59*, 822–828.

Curran, C.S., Bolig, T., and Torabi-Parizi, P. (2018). Mechanisms and targeted therapies for Pseudomonas aeruginosa lung infection. Am. J. Respir. Crit. Care Med. *197*, 708–727.

Gao, D., Wu, J., Wu, Y.T., Du, F., Aroh, C., Yan, N., Sun, L., and Chen, Z.J. (2013). Cyclic GMP-AMP synthase is an innate immune sensor of HIV and other retroviruses. Science *341*, 903–906.

Grootjans, J., Kaser, A., Kaufman, R.J., and Blumberg, R.S. (2016). The unfolded protein response in immunity and inflammation. Nat. Rev. Immunol. *16*, 469–484.

Guimaraes, E.S., Gomes, M.T.R., Campos, P.C., Mansur, D.S., Dos Santos, A.A., Harms, J., Splitter, G., Smith, J.A., Barber, G.N., and Oliveira, S.C. (2019). Brucella abortus cyclic dinucleotides trigger STING-dependent unfolded protein response that favors bacterial replication. J. Immunol. *202*, 2671–2681.

Hansen, K., Prabakaran, T., Laustsen, A., Jorgensen, S.E., Rahbaek, S.H., Jensen, S.B., Nielsen, R., Leber, J.H., Decker, T., Horan, K.A., et al. (2014). Listeria monocytogenes induces IFNbeta expression through an IFI16-, cGAS- and STING-dependent pathway. EMBO J. *33*, 1654–1666.

Huang, X., Barrett, R.P., McClellan, S.A., and Hazlett, L.D. (2005). Silencing Toll-like receptor-9 in Pseudomonas aeruginosa keratitis. Invest. Ophthalmol. Vis. Sci. *46*, 4209–4216.

Lahaye, X., Satoh, T., Gentili, M., Cerboni, S., Conrad, C., Hurbain, I., El Marjou, A., Lacabaratz, C., Lelievre, J.D., and Manel, N. (2013). The capsids of HIV-1 and HIV-2 determine immune detection of the viral cDNA by the innate sensor cGAS in dendritic cells. Immunity *39*, 1132–1142.

Li, X., Shu, C., Yi, G., Chaton, C.T., Shelton, C.L., Diao, J., Zuo, X., Kao, C.C., Herr, A.B., and Li, P. (2013). Cyclic GMP-AMP synthase is activated by double-stranded DNA-induced oligomerization. Immunity *39*, 1019–1031.

Liu, Y.P., Zeng, L., Tian, A., Bomkamp, A., Rivera, D., Gutman, D., Barber, G.N., Olson, J.K., and Smith, J.A. (2012). Endoplasmic reticulum stress regulates the innate immunity critical transcription factor IRF3. J. Immunol. *189*, 4630–4639.

Lovewell, R.R., Patankar, Y.R., and Berwin, B. (2014). Mechanisms of phagocytosis and host clearance of Pseudomonas aeruginosa. Am. J. Physiol. Lung Cell. Mol. Physiol. *306*, L591–L603.

Ma, Z., Jacobs, S.R., West, J.A., Stopford, C., Zhang, Z., Davis, Z., Barber, G.N., Glaunsinger, B.A., Dittmer, D.P., and Damania, B. (2015). Modulation of the cGAS-STING DNA sensing pathway by gammaherpesviruses. Proc. Natl. Acad. Sci. U S A *112*, E4306–E4315.

Manzanillo, P.S., Shiloh, M.U., Portnoy, D.A., and Cox, J.S. (2012). Mycobacterium tuberculosis activates the DNA-dependent cytosolic surveillance pathway within macrophages. Cell Host Microbe *11*, 469–480.

McArthur, K., Whitehead, L.W., Heddleston, J.M., Li, L., Padman, B.S., Oorschot, V., Geoghegan, N.D., Chappaz, S., Davidson, S., San Chin, H., et al. (2018). BAK/BAX macropores facilitate mitochondrial herniation and mtDNA efflux during apoptosis. Science *359*, eaao6047.

Miyoshi-Akiyama, T., Tada, T., Ohmagari, N., Viet Hung, N., Tharavichitkul, P., Pokhrel, B.M., Gniadkowski, M., Shimojima, M., and Kirikae, T. (2017). Emergence and spread of epidemic multidrug-resistant Pseudomonas aeruginosa. Genome Biol. Evol. *9*, 3238–3245.

Moretti, J., Roy, S., Bozec, D., Martinez, J., Chapman, J.R., Ueberheide, B., Lamming, D.W., Chen, Z.J., Horng, T., Yeretssian, G., et al. (2017). STING senses microbial viability to orchestrate stress-mediated autophagy of the endoplasmic reticulum. Cell *171*, 809–823.e3.

Pang, Z., Raudonis, R., Glick, B.R., Lin, T.J., and Cheng, Z. (2019). Antibiotic resistance in Pseudomonas aeruginosa: mechanisms and alternative therapeutic strategies. Biotechnol. Adv. *37*, 177–192.

Parker, D., Cohen, T.S., Alhede, M., Harfenist, B.S., Martin, F.J., and Prince, A. (2012). Induction of type I interferon signaling by Pseudomonas aeruginosa is diminished in cystic fibrosis epithelial cells. Am. J. Respir. Cell Mol. Biol. *46*, 6–13.

Parker, D., and Prince, A. (2011). Type I interferon response to extracellular bacteria in the airway epithelium. Trends Immunol. *32*, 582–588.

Petrasek, J., Iracheta-Vellve, A., Csak, T., Satishchandran, A., Kodys, K., Kurt-Jones, E.A., Fitzgerald, K.A., and Szabo, G. (2013). STING-IRF3 pathway links endoplasmic reticulum stress with hepatocyte apoptosis in early alcoholic liver disease. Proc. Natl. Acad. Sci. U S A *110*, 16544–16549.

Richardson, C.E., Kooistra, T., and Kim, D.H. (2010). An essential role for XBP-1 in host protection against immune activation in C. elegans. Nature *463*, 1092–1095.

Sadikot, R.T., Blackwell, T.S., Christman, J.W., and Prince, A.S. (2005). Pathogen-host interactions in Pseudomonas aeruginosa pneumonia. Am. J. Respir. Crit. Care Med. *171*, 1209–1223.

Sana, T.G., Baumann, C., Merdes, A., Soscia, C., Rattei, T., Hachani, A., Jones, C., Bennett, K.L., Filloux, A., Superti-Furga, G., et al. (2015). Internalization of Pseudomonas aeruginosa strain PAO1 into epithelial cells is promoted by interaction of a T6SS effector with the microtubule network. mBio *6*, e00712.

Sana, T.G., Hachani, A., Bucior, I., Soscia, C., Garvis, S., Termine, E., Engel, J., Filloux, A., and Bleves, S. (2012). The second type VI secretion system of Pseudomonas aeruginosa strain PAO1 is regulated by quorum sensing and Fur and modulates internalization in epithelial cells. J. Biol. Chem. *287*, 27095–27105.

Sun, B., Sundstrom, K.B., Chew, J.J., Bist, P., Gan, E.S., Tan, H.C., Goh, K.C., Chawla, T., Tang, C.K., and Ooi, E.E. (2017). Dengue virus activates cGAS through the release of mitochondrial DNA. Sci. Rep. *7*, 3594.

Sun, L., Wu, J., Du, F., Chen, X., and Chen, Z.J. (2013). Cyclic GMP-AMP synthase is a cytosolic DNA sensor that activates the type I interferon pathway. Science *339*, 786–791.

van 't Wout, E.F., van Schadewijk, A., van Boxtel, R., Dalton, L.E., Clarke, H.J., Tommassen, J., Marciniak, S.J., and Hiemstra, P.S. (2015). Virulence factors of Pseudomonas aeruginosa induce both the unfolded protein and integrated stress responses in airway epithelial cells. PLoS Pathog. *11*, e1004946.

Wang, L., Wen, M., and Cao, X. (2019). Nuclear hnRNPA2B1 initiates and amplifies the innate

immune response to DNA viruses. Science *365*, eaav0758.

Wassermann, R., Gulen, M.F., Sala, C., Perin, S.G., Lou, Y., Rybniker, J., Schmid-Burgk, J.L., Schmidt, T., Hornung, V., Cole, S.T., et al. (2015). Mycobacterium tuberculosis differentially activates cGAS- and inflammasome-dependent intracellular immune responses through ESX-1. Cell Host Microbe *17*, 799–810.

Watson, R.O., Bell, S.L., MacDuff, D.A., Kimmey, J.M., Diner, E.J., Olivas, J., Vance, R.E., Stallings, C.L., Virgin, H.W., and Cox, J.S. (2015). The cytosolic sensor cGAS detects Mycobacterium tuberculosis DNA to induce type I interferons and activate autophagy. Cell Host Microbe *17*, 811–819.

Wu, J., Chen, Y.J., Dobbs, N., Sakai, T., Liou, J., Miner, J.J., and Yan, N. (2019). STING-mediated disruption of calcium homeostasis chronically activates ER stress and primes T cell death. J. Exp. Med. *216*, 867–883.

Wu, J., and Chen, Z.J. (2014). Innate immune sensing and signaling of cytosolic nucleic acids. Annu. Rev. Immunol. *32*, 461–488.

Wu, J., Sun, L., Chen, X., Du, F., Shi, H., Chen, C., and Chen, Z.J. (2013). Cyclic GMP-AMP is an endogenous second messenger in innate immune signaling by cytosolic DNA. Science *339*, 826–830.

Yamashiro, L.H., Wilson, S.C., Morrison, H.M., Karalis, V., Chung, J.J., Chen, K.J., Bateup, H.S., Szpara, M.L., Lee, A.Y., Cox, J.S., et al. (2020). Interferon-independent STING signaling promotes resistance to HSV-1 in vivo. Nat. Commun. *11*, 3382.

Yanai, H., Negishi, H., and Taniguchi, T. (2012). The IRF family of transcription factors: inception, impact and implications in oncogenesis. Oncoimmunology *1*, 1376–1386.

Zheng, Y., Liu, Q., Wu, Y., Ma, L., Zhang, Z., Liu, T., Jin, S., She, Y., Li, Y.P., and Cui, J. (2018). Zika virus elicits inflammation to evade antiviral response by cleaving cGAS via NS1-caspase-1 axis. EMBO J. *37*, e99347.

iScience, Volume *24*

Supplemental Information

Identification of cGAS as an innate immune sensor of extracellular bacterium *Pseudomonas aeruginosa*

Chuan-min Zhou, Biao Wang, Qun Wu, Ping Lin, Shu-gang Qin, Qin-qin Pu, Xue-jie Yu, and Min Wu

Transparent Methods

Ethics statement

This study followed the recommendations of the Guide for the Care and Use of Laboratory Animals of the National Institutes of Health. All mice protocols were approved by the Institutional Animal Care and Use Committee (IACUC) at the University of North Dakota (Assurance Number: A3917-01).

Mice

C57BL/6J mice and *STING*$^{-/-}$ mice (8-12 weeks) were obtained from Jackson Laboratory (Bar Harbor, ME). *cGAS*$^{-/-}$ mice (C57BL/6J background) were kindly provided by H. W. Virgin (WASH U) and Charles M Rice (Rockefeller Univ.). Mice were anesthetized using ketamine and xylazine (45 mg/kg and 10 mg/kg). For lung infection model, mice were instilled intranasally with 0.5×10^7 CFU *P. aeruginosa* (six mice/group). Mice were monitored for symptoms every day. Mice were maintained in a specific pathogen free animal facility at the University of North Dakota and Wuhan University.

Primary cells and cell lines

MH-S, RAW264.7, THP-1 cells were kept in our laboratories. BMDMs, AMs and PMs were generated from wild-type C57BL/6 and *cGAS*$^{-/-}$ mice. Macrophages were cultured in RMPI 1640 + 10% FBS + 20 mM HEPES + 2 mM L-glutamine. Primary BMDMs were grown for 10 days stimulated with 25 ng/ml M-CSF. Epithelial cells were cultured in DMEM. The differentiation of THP-1 monocytes into macrophages is conducted at a concentration of 100ng/ml PMA for 48 hours.

Plasmids construction

To construct the mouse *BiP* and *ATF4* promoter luciferase plasmids, the *BiP* (-700 to -400) and *ATF4* (-590 to -290) promoter fragments were amplified from the RAW264.7 cell genome by PCR, then sub-cloned into the *Kpn*I and *Hind*III sites of pGL3-Enhancer Vector (Promega, WI). To construct pET-28a-mcGAS plasmids, cDNA fragments were amplified from BMDMs cDNA with its specific primer and cloned into *Sal*I and *Xho*I sites of the pET-28a vector (Millipore, MA).

Constructed plasmids were transformed into *Escherichia coli* BL21(DE3) (New England Biolabs, MA). PCR primers were shown in Supplemental Table 1.

Generation of gene knockout cell lines

For targeting with CRISPR/Cas9, we used a lentiCRISPR v2 to construct cGAS and STING KO cells. Guide RNA sequences (cGAS: 5′ - CACCG GCTGGAGCCTCCTGCGGCT -3′; STING: 5′ - CACCGCAGGCACTCAGCAGA ACCA -3′). The cGAS or STING lentiCRISPR v2 plasmid and packaging plasmids pVSVg and psPAX2 were co-transfected into HEK293T cells. The cellular supernatants were collected to generate "lentiCRISPR v2" lentivirus. cGAS and STING KO cells were selected with 1 μg/ml puromycin for 7 days followed by 24 h lentivirus treatment.

Bacterial strains

Pseudomonas aeruginosa PAO1, PAO1-GFP, PAO1-mCherry, *K. pneumoniae* and *S. aureus* were cultured in LB broth and agar plates at 37°C. As for invitro infection, bacteria were cultured for 16 h in LB broth medium and then pelleted by centrifugation at 5000g. Cells were then cultured to antibiotic-free medium and infected with bacteria at MOI of 10 for 1 to 4 hours.

RNA isolation and quantitative real-time PCR

Cells were collected in Trizol and RNA was isolated following the manufacturer's instructions. cDNA was synthesized using the High Capacity cDNA Reverse Transcription Kit (Thermo, MA). qPCR was performed using SYBR Green qPCR Master Mix (Thermo) and gene-specific primers (Supplemental Table 1). mRNA levels were normalized to *β-actin*.

Isolation and transfections of *P. aeruginosa* DNA

P. aeruginosa was grown in LB broth with or without 1.2mM EdU. *P. aeruginosa* genomic DNA was isolated using GeneJET Genomic DNA Purification Kit (Thermo). ISD oligos were annealed in 5 mM Tris + 25 mM NaCl buffer at 98°C for 5 min and then cooling to room temperature for 1 h. Cells were transfected with 2 μg of annealed ISD oligos or *P. aeruginosa* DNA using lipofectamine 3000 (Invitrogen). Cells were harvested after 8 h transfection.

ChIP-PCR

ChIP-PCR was performed using Pierce™ Agarose ChIP Kit (Thermo) following the

manufacturer's instructions. BMDMs were crosslinked with 1% formaldehyde for 10 min at room temperature. Samples were then washed with cold PBS and lysed in the lysis buffer with protease inhibitors. DNA was lysed into the desired fragment length (200 to 600bp) using Micrococcal Nuclease for 15 min at 37°C water bath. Equal amounts of DNA were immunoprecipitated using IgG, IRF3 antibodies. Immunoprecipitated and input DNA was eluted and amplified with primers for UPR molecules (Supplemental Table 1). To relate our studies to the existing data, we downloaded BED files containing the enrichment of IRF3-ChIP binding sites and STAT1-ChIP binding sites from GEO database (GEO Accession number: GSM2698322, GSM925279, GSM1356204, GSM1356222) (Mancino et al., 2015; Purbey et al., 2017). ChIP data were visualized by Integrative Genomics Viewer.

cGAS protein purification

BL21(DE3) transformed with pET-28a-cGAS was cultured in LB medium with kanamycin at 37°C. The cGAS protein was induced with 1 mM Isopropyl β-D-1-thiogalactopyranoside (IPTG) at 16°C for 16 h. The His-tagged protein was purified using Ni-NTA beads. The protein was identified by SDS-PAGE and immunoblotting. hcGAS protein was ordered from NOVUS Biologicals (CO).

Electrophoretic molecular shift assay (EMSA)

Pseudomonas rrs gene probes were amplified by PCR and purified using GeneJet Gel Extraction and DNA Cleanup Micro Kit (Thermo). Briefly, cGAS proteins were mixed with these probes following the EMSA kit (Thermo) manufacturer's instructions and incubated at room temperature for 20 min. The cGAS-probe mixtures were then analyzed by 5% native PAGE gel and electrophoresed in 0.5X TBE buffer at 90V for 90 min. The gels were then stained with SYBR Green EMSA Nucleic Acid Gel Stain.

Co-immunoprecipitation

RAW267.4 cells were infected with *P. aeruginosa*, washed with cold PBS, fixed in 4% PFA and then quenched with 1 M Tris (pH 7.4). Next, cells were lysed using lysis buffer followed by sonication using sonicator in water bath. Samples were then immunoprecipitated with protein A/G

Magnetic Beads pre-cross-linked with cGAS antibody. IP efficiency was detected with Western blot analysis. Samples were de-crosslinked at 65°C for 16 h and then treated with proteinase K. DNA was isolated using Trizol and resuspended in 10 mM Tris. qPCR was then performed to measure the abundance of relevant genes (Watson et al., 2015). All primers were shown in Supplemental Table 1.

Western blotting

Primary antibodies using for immunoblotting: antibodies against cGAS, STING, TBK1, IRF3, p-IRF3, BiP, PERK, ATF4, CHOP, IRE1, XBP1, STAT1, p-STAT1, Histone H3, IRF9 and STAT2 were obtained from Cell Signaling Technology, p-STAT2 (Millipore, MA), p-PERK, ATF6, and β-actin were purchased from Santa Cruz. p-IRE1, mouse and rabbit second antibodies using for immunoblotting were ordered from Invitrogen. Briefly, the cell or tissue samples were lysed in RIPA with protease inhibitor (Roche Diagnostics, IN) for 30 min on ice and then quantitated. SDS Loading Buffer was added into the sample supernatants and then boiled for 10 min at 95°C. 20 μg proteins of each sample were loaded and separated by 10-15% SDS-PAGE gels and transferred onto nitrocellulose and blocked for 1 h at room temperature using 5% nonfat milk. After that, the membranes were incubated using primary Abs overnight at 4°C and second antibody for 2 h. Protein bands were visualized using an enhanced chemiluminescence detection kit and quantified by Quantity One software.

ELISA

IFN-α, IFN-β levels in cell culture supernatants, lung tissues, BALFs, and bloods were detected using mouse IFN-α, IFN-β ELISA Kit (R&D Systems, CO). Briefly, precoated ELISA plates were incubated with 100μL diluted samples, antibody solution, and HRP Solution respectively. PBST was used as wash buffer, each incubation was followed by PBST for 4 times. Lastly, 100 μl of the TMB Substrate Solution was added to each well, incubated 15 min in the dark, and blocked by 100 μl of Stop Solution. Microplate reader was used to determine the absorbance at 450 nm within 5 minutes after the addition of the Stop Solution.

Bacterial burden assay

AMs from BALF, and tissues were homogenized with PBS. CFU were measured using LB agar plates (Guo et al., 2012).

Immunofluorescence

The cells were washed with PBS, fixed in 4% paraformaldehyde for 20 min and then permeabilized with 0.5% Triton X-100 for 20 min. After blocked with 5% non-fat milk for 30 min, the cells were incubated with first antibody and second antibody (diluted by 2% BSA) at 4°C. Nuclear was stained using DAPI. Images were observed under an LSM 510 Meta Confocal Microscope.

Histological analysis

Tissues were fixed in 10% formalin for 24 hours, embedded in paraffin and then processed for H&E staining (AML laboratories, FL).

Statistical analysis

Most experiments were performed for 3 times. One-way ANOVA (Tukey post hoc test) was used for data analysis in GraphPad Prism 7. Besides, survival rates were calculated using Kaplan–Meier curve. ChIP-seq data reported in this paper are from GEO database: IRF3 ChIP (GEO Accession number: GSM2698322, GSM925279), STAT1 ChIP (GEO Accession number: GSM1563689, GSM1563692).

Supplemental Figures and legends

FIGURE S1

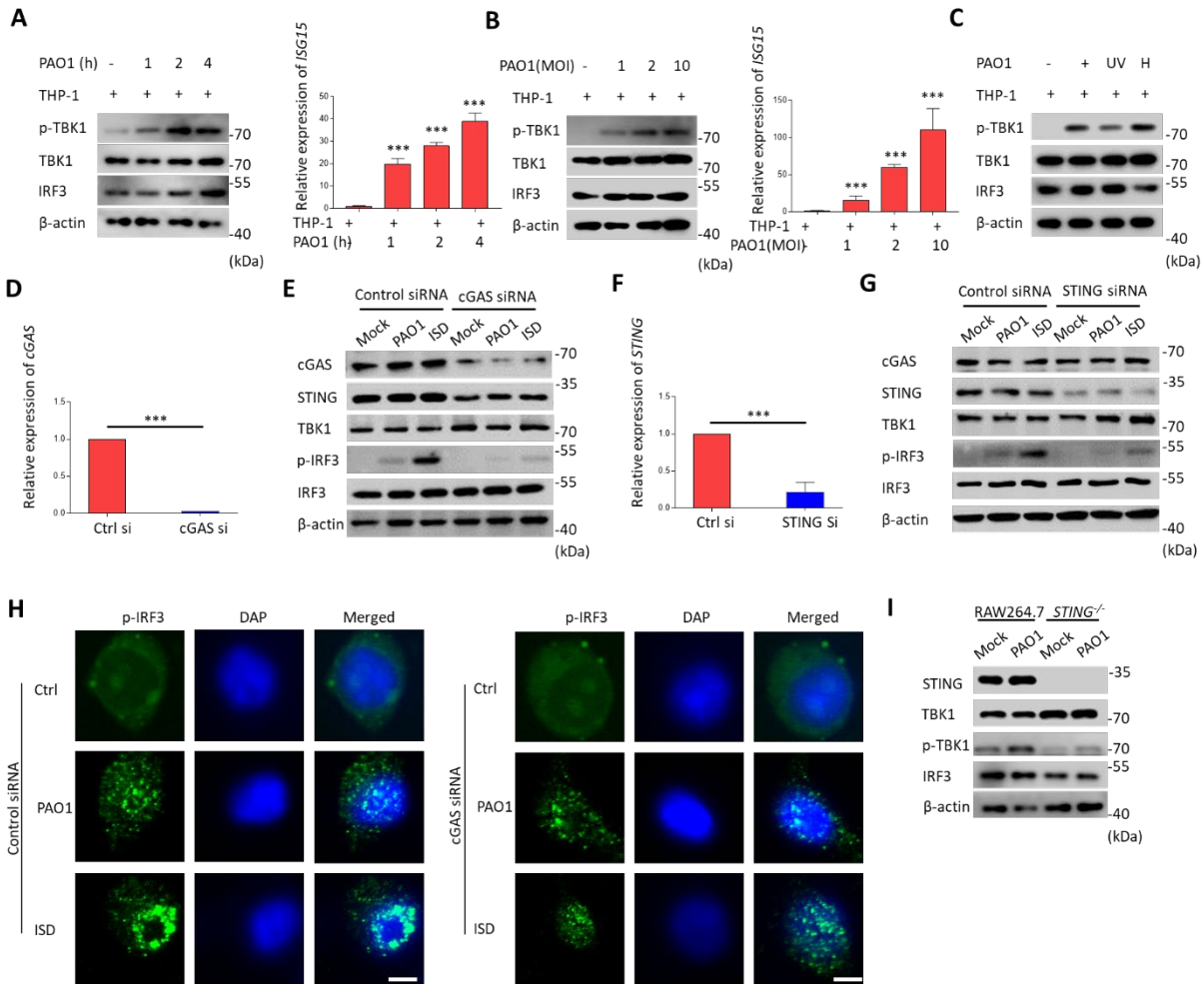

S1 Fig. *P. aeruginosa* activated cGAS signaling pathways, related to Figure 1

(A) THP-1 cells were treated with 10 MOI *P. aeruginosa* for 1, 2, or 4 h. Immunoblot analysis of cGAS signaling pathways.

(B) THP-1 cells were treated with 1, 2, or 10 MOI *P. aeruginosa* for 4 h. Immunoblot analysis of cGAS signaling pathways.

(C) THP-1 cells were treated with 10 MOI *P. aeruginosa*, UV-*P. aeruginosa*, or Heated- *P. aeruginosa* for 4 h. Immunoblot analysis of cGAS signaling pathways.

(D) RAW264.7 cells were transfected with control siRNA or cGAS siRNA for 48 h, and qPCR analysis of mRNA levels of *cGAS*.

(E) RAW264.7 cells were transfected with control siRNA or cGAS siRNA and then treated with 10 MOI *P. aeruginosa* or ISD for 4 h. Immunoblot analysis of cGAS signaling pathways.

(F) RAW264.7 cells were transfected with control siRNA or STING siRNA for 48 h, and qPCR analysis of mRNA levels of *STING*.

(G) RAW264.7 cells were transfected with control siRNA or STING siRNA and then treated with 10 MOI *P. aeruginosa* or ISD for 4 h. Immunoblot analysis of cGAS signaling pathways.

(H) *STING*$^{-/-}$ RAW264.7 cells were treated with 10 MOI *P. aeruginosa* for 4 h. Immunoblot analysis of cGAS signaling pathways.

(I) RAW264.7 cells were transfected with control siRNA or cGAS siRNA and then treated with 10 MOI *P. aeruginosa* or ISD for 4 h. Immunofluorescence detecting nuclear translocation of IRF3. Scale bar, 5 μm.

qPCR Data (mean ± SEM) are representative of three independent experiments. ($*p \leq 0.05$, $**p \leq 0.01$, $***p \leq 0.001$ one-way ANOVA with Tukey post hoc test)

FIGURE S2

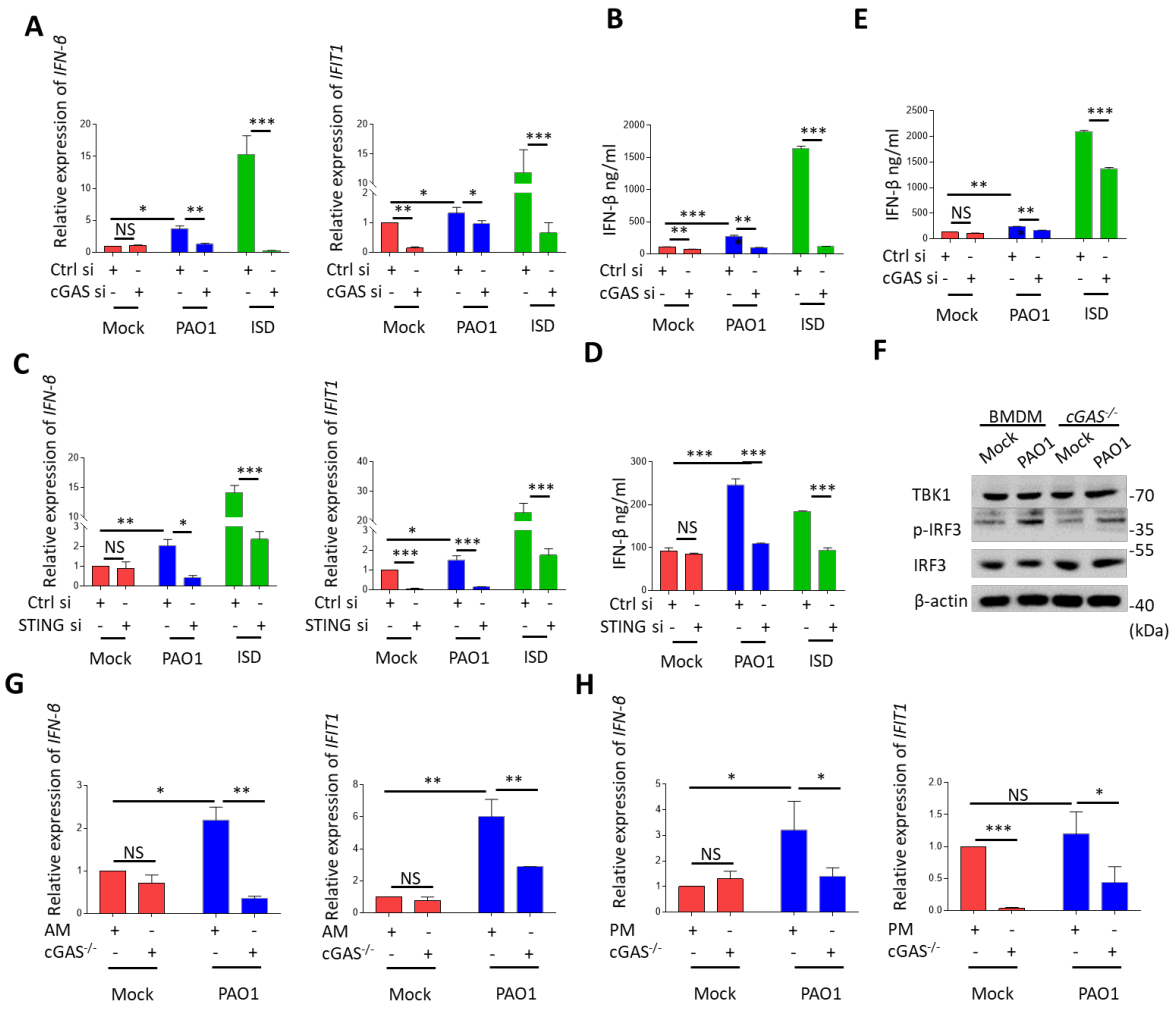

S2 Fig. *P. aeruginosa* activated cGAS signaling pathways in macrophages, related to Figure 1

(A) RAW264.7 cells were transfected with control siRNA or cGAS siRNA and then treated with 10 MOI *P. aeruginosa* or ISD for 4 h. qPCR was performed to measure mRNA levels of *IFN-β* or *IFIT1*.

(B) RAW264.7 cells were transfected with control siRNA or cGAS siRNA or STING siRNA and then treated with 10 MOI *P. aeruginosa* or ISD for 4 h. Cytokine levels of IFN-β in cell culture supernatant were detected using ELISA.

(C) RAW264.7 cells were transfected with control siRNA or STING siRNA and then treated with 10 MOI *P. aeruginosa* or ISD for 4 h. qPCR was performed to measure mRNA levels of *IFN-β* or *IFIT1*.

(D) RAW264.7 cells were transfected with control siRNA or STING siRNA and then treated with 10 MOI *P. aeruginosa* or ISD for 4 h. Cytokine levels of IFN-β in cell culture supernatant were detected using ELISA.

(E) MH-S cells were transfected with control siRNA or cGAS siRNA and then treated with 10 MOI *P. aeruginosa* or ISD for 4 h. Cytokine levels of IFN-β were measured by ELISA.

(F) WT and *cGAS*$^{-/-}$ BMDMs were treated with 10 MOI *P. aeruginosa* or ISD for 4 h. Immunoblotting analysis of cGAS signaling pathways.

(G) WT and *cGAS*$^{-/-}$ alveolar macrophages were treated with 10 MOI *P. aeruginosa* or ISD for 4 h. qPCR was performed to measure mRNA levels of *IFN-β* or *IFIT1*.

(H) WT and *cGAS*$^{-/-}$ peritoneal macrophages were treated with 10 MOI *P. aeruginosa* or ISD for 4 h. qPCR was performed to measure mRNA levels of *IFN-β* or *IFIT1*.

qPCR and ELISA Data (mean ± SEM) are representative of three independent experiments. (*$p \leq 0.05$, **$p \leq 0.01$, ***$p \leq 0.001$ one-way ANOVA with Tukey post hoc test)

FIGURE S3

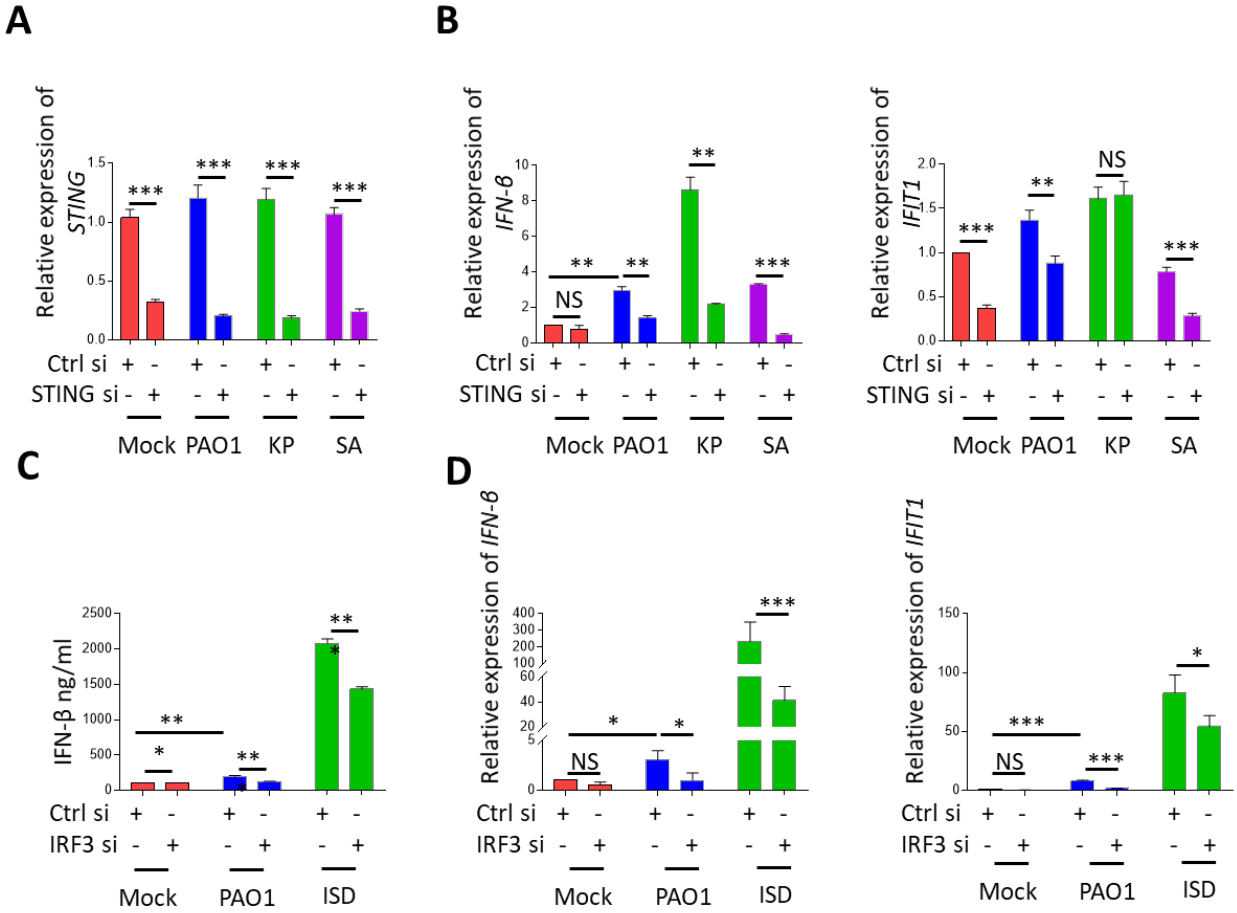

S3 Fig. cGAS signaling pathway is responsible for detecting extracellular bacteria, related to Figure 1

(A) BMDMs were transfected with control siRNA or STING siRNA for 48 h and then infected with 10 MOI *P. aeruginosa*, *K. pneumoniae*, and *S. aureus* for 4 h in BMDMs. qPCR analysis of mRNA levels of *STING*.

(B) BMDMs were transfected with control siRNA or STING siRNA for 48 h and then infected with 10 MOI *P. aeruginosa*, *K. pneumoniae*, and *S. aureus* for 4 h in BMDMs. qPCR analysis of mRNA levels of *IFN-β* or *IFIT1*.

(C) RAW264.7 cells were transfected with control siRNA or IRF3 siRNA and then treated with 10 MOI *P. aeruginosa* or ISD for 4 h. Cytokine levels of IFN-β in cell culture supernatant were detected using ELISA.

(D) RAW264.7 cells were transfected with control siRNA or IRF3 siRNA and then treated with 10 MOI *P. aeruginosa* or ISD for 4 h. qPCR was performed to measure mRNA levels of *IFN-β* or *IFIT1*.

qPCR and ELISA Data (mean ± SEM) are representative of three independent experiments. (*$p \leq 0.05$, **$p \leq 0.01$, ***$p \leq 0.001$ one-way ANOVA with Tukey post hoc test)

FIGURE S4

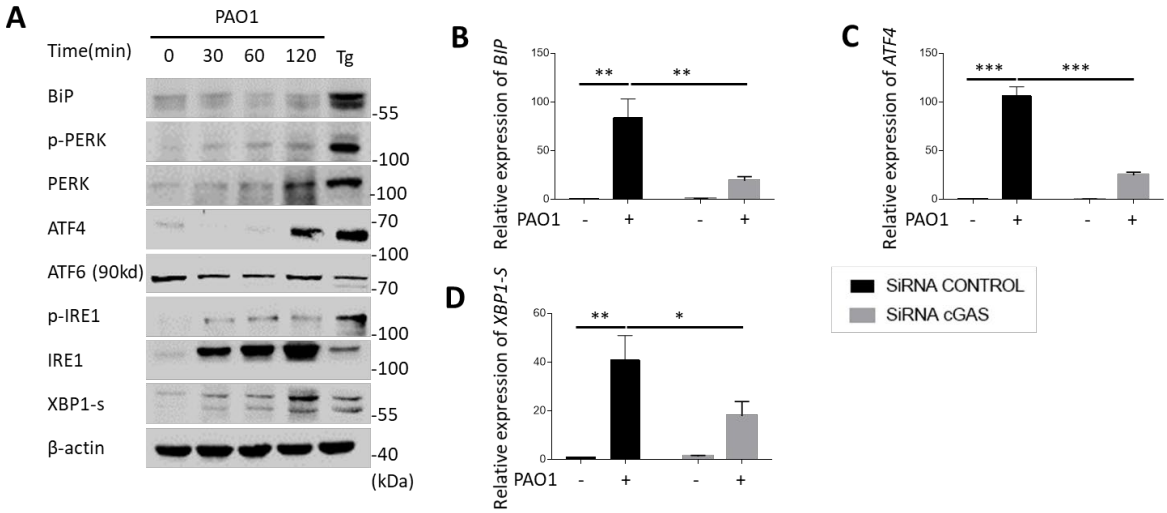

S4 Fig. UPR is activated under *P. aeruginosa* infection, related to Figure 3

(A) WT alveolar macrophages were infected with 20 MOI *P. aeruginosa* for 0.5, 1, or 2h, and Immunoblot analysis of UPR signaling pathways.

(B-D) RAW264.7 cells were transfected with control siRNA or cGAS siRNA for 48 h, and then treated with 10 MOI *P. aeruginosa* or ISD for 4 h. qPCR measuring mRNA levels of *BiP*, *ATF4*, and *XBP1-s*.

qPCR Data (mean ± SEM) are representative of three independent experiments. (*$p \leq 0.05$, **$p \leq 0.01$, ***$p \leq 0.001$ one-way ANOVA with Tukey post hoc test)

FIGURE S5

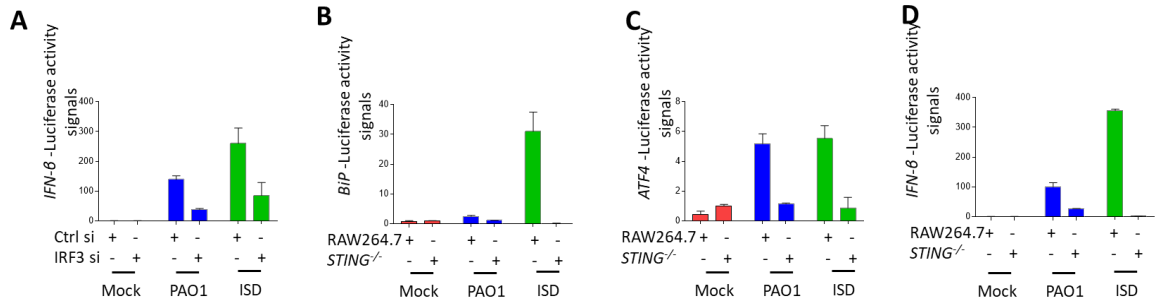

S5 Fig. *P. aeruginosa* activated IFN-dependent UPR, related to Figure 4

(A) Control siRNA or IRF3 siRNA-treated RAW264.7 cells were pre-transfected with *IFN-β* luciferase vectors for 24 h and then treated with 10 MOI *P. aeruginosa* or ISD for 4 h. Luciferase activity were detected using Dual-Luciferase Reporter Assay System.

(B) *STING*$^{-/-}$ RAW264.7 cells were were pre-transfected with *BiP*, *ATF4* and *IFN-β* luciferase vectors for 24 h and then treated with 10 MOI *P. aeruginosa* for 4 or ISD for 4 h. Luciferase activity were detected using Dual-Luciferase Reporter Assay System.

FIGURE S6

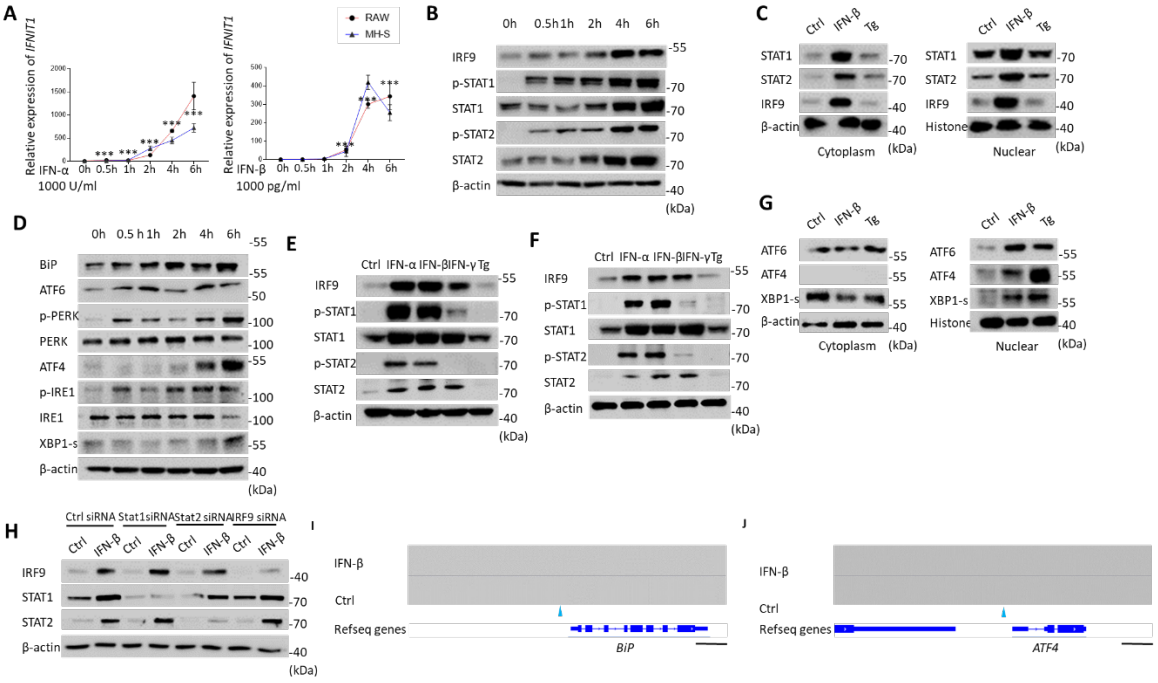

S6 Fig. *P. aeruginosa* activated IFN-dependent UPR, related to Figure 4

(A) RAW264.7 and MH-S cells were treated with IFN-α or IFN-β at different time points and then detected mRNA levels of *IFIT1*.

(B) RAW264.7 cells were treated with IFN-β at different time points. Immunoblotting analysis of JAK-STAT signaling pathways.

(C) RAW264.7 cells were treated with IFN-β or Tg for 6h. Immunoblotting analysis of STAT1, STAT2 and IRF9 in cytoplasmic and nuclear fractions of RAW264.7 cells.

(D) RAW264.7 cells were treated with IFN-β at different time points. Immunoblotting analysis of UPR signaling pathways.

(E) RAW264.7 cells were treated with IFN-α, IFN-β, IFN-γ and Tg for 6h. Immunoblotting analysis of JAK-STAT signaling pathways.

(F) BMDMs were treated with IFN-α, IFN-β, IFN-γ and Tg for 6h. Immunoblotting analysis of JAK-STAT signaling pathways.

(G) RAW264.7 cells were treated with IFN-β or Tg for 6h. Immunoblotting analysis of ATF6, ATF4 and XBP1 in cytoplasmic and nuclear fractions of RAW264.7 cells.

(H) RAW264.7 cells were transfected with control siRNA, STAT1 siRNA, STAT2 siRNA and IRF9 siRNA IFN-β for 48h and then treated with IFN-β for 6h. Immunoblotting analysis of JAK-STAT signaling pathways.

(I, J) Chromatin immunoprecipitation sequencing (ChIP-seq) for STAT1 binding in BiP, ATF4 normalized by input. Blue arrows indicate transcription start site (TSS) of *BiP* or *ATF4*. Scale bar 1000bp.

qPCR Data (mean ± SEM) are representative of three independent experiments. (*$p \leq 0.05$, **$p \leq 0.01$, ***$p \leq 0.001$ one-way ANOVA with Tukey post hoc test)

FIGURE S7

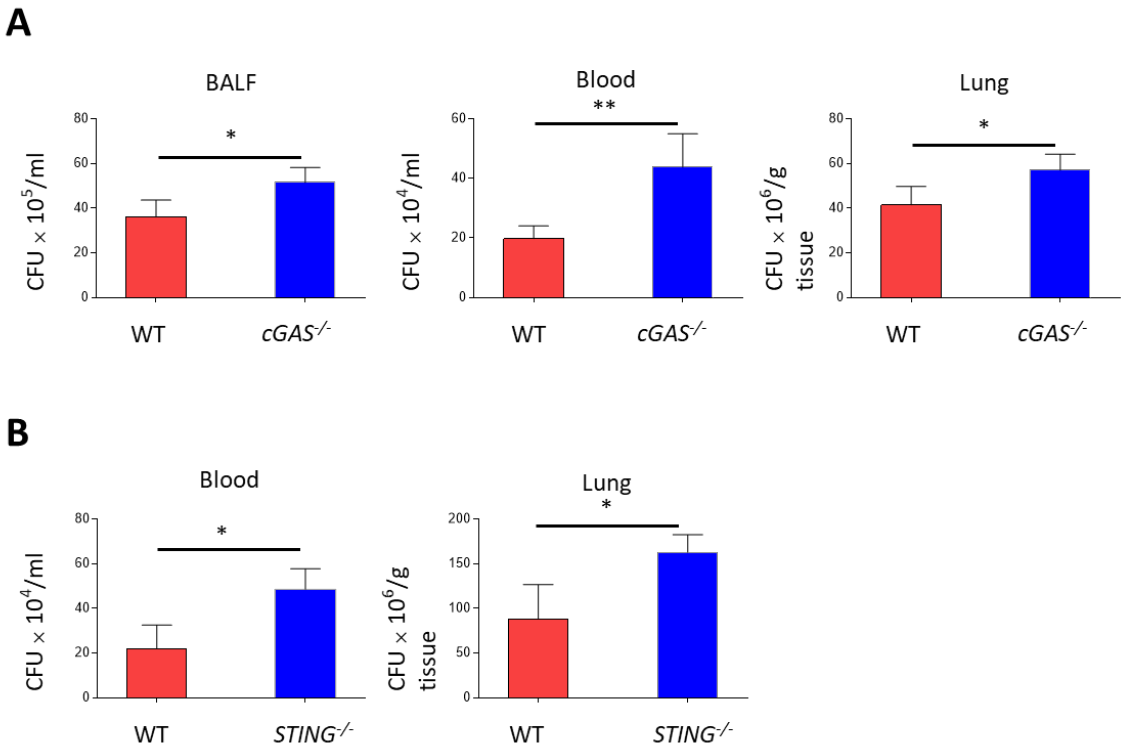

S7 Fig. The cGAS signaling pathway modulates bacterial burdens under *P. aeruginosa* infection, related to Figure 5

(A) Bacterial burdens of *P. aeruginosa* in BALF, blood and lung were detected after 24 h post *P. aeruginosa* infection in *cGAS*$^{-/-}$ mice compared with WT mice.

(**B**) Bacterial burdens of *P. aeruginosa* in blood and lung were detected after 24 h post *P. aeruginosa* infection in *cGAS*$^{-/-}$ mice compared with WT mice.

CFU (mean ± SEM) are representative of three independent experiments. (*$p \leq 0.05$, **$p \leq 0.01$, ***$p \leq 0.001$ one-way ANOVA with Tukey post hoc test)

Supplemental References

Guo, Q., Shen, N., Yuan, K., Li, J., Wu, H., Zeng, Y., Fox, J., 3rd, Bansal, A.K., Singh, B.B., Gao, H., et al. (2012). Caveolin-1 plays a critical role in host immunity against Klebsiella pneumoniae by regulating STAT5 and Akt activity. European journal of immunology *42*, 1500-1511.

Mancino, A., Termanini, A., Barozzi, I., Ghisletti, S., Ostuni, R., Prosperini, E., Ozato, K., and Natoli, G. (2015). A dual cis-regulatory code links IRF8 to constitutive and inducible gene expression in macrophages. Genes & development *29*, 394-408.

Purbey, P.K., Scumpia, P.O., Kim, P.J., Tong, A.J., Iwamoto, K.S., McBride, W.H., and Smale, S.T. (2017). Defined Sensing Mechanisms and Signaling Pathways Contribute to the Global Inflammatory Gene Expression Output Elicited by Ionizing Radiation. Immunity *47*, 421-434 e423.

Watson, R.O., Bell, S.L., MacDuff, D.A., Kimmey, J.M., Diner, E.J., Olivas, J., Vance, R.E., Stallings, C.L., Virgin, H.W., and Cox, J.S. (2015). The Cytosolic Sensor cGAS Detects Mycobacterium tuberculosis DNA to Induce Type I Interferons and Activate Autophagy. Cell host & microbe *17*, 811-819.